

Politecnico di Torino

Master of Science

Academic Year 2025/2026

Graduation Session September 2026

3D Printable Bio–based Vitrimer Resins

Advisors:

Camilla Noe'

Massimo Messori

Candidate:

Halil Ibrahim Karakis

Table of contents

List of figures……....VII

List of tables……X

Abstract...……..XII

Acknowledgements……..XV

Chapter 1: Introduction……1

1.1 Vitrimers: Mechanisms of vitrimers, bio–based sources……1

1.2 Processing and manufacturing methods of vitrimers……3

Chapter 2: Bio–based vitrimer formulations……...5

2.1. 3D Printed Bio–based vitrimer formulations……...…….5

2.1.1 Transesterification……...5

2.1.1.1 GDGDA–THFMA……6

2.1.1.2 DGEVADMA–HPPA……...7

2.1.1.3 HPPA–MCC……...10

2.1.1.4 AESO–AEUG–EUGP……11

2.1.1.5 THFMA–AESO–HPPA……..13

2.1.1.6 DPEPA–GDGDA–GLYFOMA–RTE……..……...14

2.1.1.7 HPPA–AESO……..16

2.1.1.8 AERO–HPPA–GDGDA……17

2.1.1.9 AELO–EGMP–TMP3MP–DMEP……18

2.1.2 Imine bonds……...20

2.1.2.1 HMDA–MAV–EGPMA……20

2.1.2.2 CROSS–BDG–IBOMA…….…….22
2.1.3 Disulfide bonds……..25
2.1.3.1 CMAV–IBA……26
2.2. Bio–based formulations not yet demonstrated by vat photopolymerization……27
2.2.1 Transesterification bonds without vat photopolymerization……..27
2.2.1.1 FEP–FEHBP–CA……...27
2.2.1.2 ESO–GL…….29
2.2.2. Imin bonds without printing…….31
2.2.2.1 PV–1071 and PV–1074……...……31
2.2.3. Disulfide bonds without vat photopolymerization……32
2.2.3.1 DGEVA–Cystamine……32
2.2.4. Boronic ester bonds without vat photopolymerization…….33
2.2.4.1 ESBO–HEA–DBDT……...……34
2.2.4.2 ESOA–DBEDT……..35
Chapter 3: Filler materials……..37
3.1 Hexagonal boron nitride (hBN)……37
3.2 Magnetite nanoparticles (Fe_3O_4)……..39
3.3 Carbon nanotubes (CNTs/MWCNTs)……..……41
3.4 Cellulose–based nanofillers (CNCs/CNFs)……..43
3.4.1 Cellulose nanocrystals (CNCs)…….……44
3.4.2 Cellulose nanofibers (CNFs)…….45
3.5 Functionalized silica…….46
3.6 Graphene oxide (GO)……48

3.7 Activated carbon……...50

3.8 Amine–functionalized POSS (POSS–NH_2)……...……...51

Chapter 4: Results and Discussion ……..54

Chapter 5: Conclusion……..58

Bibliography……..60

List of figures

Figure 1 – The mechanism of the transesterification

Figure 2 – Stress relaxation curve of GDGDA–THFMA

Figure 3 – Mechanical properties of GDGDA–THFMA

Figure 4 – Stress relaxation curve of DGEVADMA–HPPA

Figure 5 – Stress–strain graph of DGEVADMA–HPPA

Figure 6 – Mechanical properties of DGEVADMA–HPPA

Figure 7 – Stress relaxation curve of HC10

Figure 8 – Stress–relaxation graph of AESO–AEUG–EUGP with BG–Te

Figure 9 – Stress–relaxation graph of THFMA–AESO–HPPA

Figure 10 – Mechanical properties of THFMA–AESO–HPPA

Figure 11 – Stress relaxation curve of DPEPA–GDGDA–GLYFOMA–RTE

Figure 12 – Stress–relaxation graph of HPPA–AESO. The values for 140 °C, 160 °C, 180 °C, 200 °C indicates the formulation 90 wt% HPPA and 10 wt% AESO. 0HPPA represents 100 wt% AESO and 9HPPAV represents post cured vitrimer at 200 °C for 4 h.

Figure 13 – A)Transimination B)Imine methathesis

Figure 14 – 3D printings of UV25 resin system

Figure 15 – Reaction scheme of BDG and CROSS

Figure 16 – A) Stress relaxation curve of CROSS–10 B) Stress relaxation curve of CROSS–5 C) Stress relaxation curve of CROSS–0 D) Activation energy of CROSS–0, CROSS–5 and CROSS–10

Figure 17 – A) Stress–strain graph of CROSS–10 B) Stress–strain graph of CROSS–5 C) Stress–strain graph of CROSS–0 D) Young's modulus of CROSS–0, CROSS–5 and CROSS–10 according to cycles

Figure 18 – Disulfide bonds exchange mechanism

Figure 19 – Production of FEP and FEHBP and curing the vitrimer resin

Figure 20 – Recycle scheme

Figure 21 – Curing reaction of ESO and GL

Figure 22 – Curing reaction and depolymerization of DGEVA–Cystamine

Figure 23 – Preparation of ESBO–HEA–DBDT

Figure 24 – Self–repairing performance of hBN

Figure 25 – Shematic representation of corrosion protection and self repairing via thermal activation

Figure 26 – Stress–strain curve of (i) control sample (ii) sample with hole (iii) repaired sample

Figure 27 – A) 0.5 wt% CNT before light treatment B) 0.5 wt% CNT after light treatment

Figure 28 – Self healing ability with different weight ratios

Figure 29 – Self healing mechanism with Joule heating

Figure 30 – Miling of CNC and combining with zinc acetate catalyst

Figure 31 – Illustration of CNF matrix

Figure 32 – Scheme of synthesis of functionalized silica

Figure 33 – Mechanical properties of vitrimer matrix and silica composites

Figure 34 – Healing efficency of vitrimer matrix and silica composites

Figure 35 – Flexural strength and modulus of Epoxy–GO

Figure 36 – Flexural modulus of Epoxy–GO before healing and after healing cycles

Figure 37 – Healing of epoxy vitrimer

Figure 38 – Stress–strain graph of the resins

List of tables

Table 1 – Comparison of HPPA–AESO and HPPA–AESO–THFMA

Table 2 – Formulations of AERO–HPPA–GDGDA

Table 3 – Stress relaxation table of AERO–HPPA–GDGDA with and without catalyst

Table 4 – Comparison of AELO–EGMP and AELO– TMP3MP

Table 5 – Different formulations of CROSS–BDG–IBOMA resin

Table 6 – Resin ratios of CMAV–IBA

Table 7 – Relaxation times of CA/DGEBA, CA/FEP, CA/ FEHBP

Table 8 – Relaxation times of ESO–GL

Table 9 – Approximate relaxation times of PV–1071 and PV–1074

Table 10 – Relaxation time of ESBO–HEA–DBDT

Table 11 – Mechanical properties of EP–p and EP–1

Table 12 – Different POSS–NH2 ratios in different resins

Table 13 – Summary table of vat photopolymerization resins

Table 14 – Summary table of resins without vat photopolymerization

Table 15 – Comparison of vat photopolymerization printers

Abstract

In recent years, production of thermosetting polymers are highly increased because of their particular performance such as mechanical strength, chemical and thermal stability and also low weight. However, besides these excellent features, their permanent crosslinks structures prevent reshaping and recycling. Therefore at the end of the life time most of the thermosetting polymers burnt or used as a landfills. At the same time additive manufacturing has enabled the production of complex geometries while reducing material waste. Between the all manufacturing techniques, stereolithography (SLA), digital light processing (DLP), and LCD–based printing, are promising methods because of their high printing resolution, surface quality and easy modelling. These technologies rely on photocurable resins cured by UV or visible light. Therefore biobased photocurable 3D resins systems became an important research topic.

Some bio–based vitrimer formulations combine renewable feedstocks, dynamic covalent networks, and photocurable functional groups, making them suitable for vat photopolymerization. Instead of thermosetting polymers, vitrimers have dynamic covalent bonds that can be rearranged when heat is applied while maintaining the crosslinked structure. This behavior gives vitrimers the ability to be repaired, reshaped, and welded. Several dynamic covalent chemistries, including transesterification, imine bonds, disulfide bonds, boronic ester bonds etc. have been successfully combined with bio–based materials to develop sustainable vitrimer resins. Among them, transesterification and imine bonds are commonly investigated mechanisms in vitrimer systems developed for vat photopolymerization. In addition to these, in this work potential resin systems were also investigated to evaluate their suitability for vat photopolymerization.

Besides the resin properties, filler materials are effectively used for improving vitrimer performance in different aspects. Hexagonal boron nitride (hBN) is mainly used for its thermal conductivity to support distribution of the heat inside the resin and this makes more efficient rearrangement of dynamic covalent bonds while carbon nanotubes(CNTs) provide resin to conduct electricity and provides Joule heating. In this study, various filler materials are discussed according to the different properties they provide to vitrimer systems. Some of the filler strategies discussed in this review were originally demonstrated in non–bio–based or non–vat–printed vitrimer matrices and are therefore considered as potentially transferable approaches for future printable bio–based systems.

This review explains recent developments in bio–based vitrimer formulations for vat photopolymerization, distinguishing experimentally printed systems from non–printed networks with potential for future resin development. The literature shows that transesterification is currently the most succesful exchange mechanism for printed bio–based vitrimer systems, while imine and disulfide networks offer additional routes to repair, reprocessing, and chemical recycling. Filler strategies can further improve thermal transport, electrical activation, mechanical reinforcement, or low–temperature repair, although many have not yet been demonstrated in fully bio–based vat–printable formulations. In this case, resin viscosity, photocuring efficiency, exchange temperature, and sustaining its strength after recycling are still main problems.

Acknowledgements

I would like to express my sincere gratitude to my supervisor Dr. Camilla Noè, for her continuous guidance, support, and valuable feedback throughout the development of this thesis. Her knowledge, patience, and constructive suggestions were essential in helping me overcome the challenges encountered during this research and in improving the quality of this work.

I would also like to thank Prof. Massimo Messori for his support and guidance throughout my research and for providing valuable advice. I am grateful to all the members of the research group for their help, collaboration, and for creating a positive working environment throughout my studies.

Finally, I would like to thank my friends and family for their support, patience, and encouragement throughout my master's studies, especially my parents Rustem Karakis and Ayse Karakis. Their support has been an important part of completing this thesis and reaching this stage of my academic journey.

Chapter 1: Introduction

1.1 Vitrimers: Mechanisms of vitrimers, bio–based sources

Vitrimers are permanently crosslinked polymer networks containing covalent bonds that can exchange under heat or another suitable conditions. They belong to the broader family of covalent adaptable networks (CANs). Unlike conventional thermosets, their internal network can rearrange without losing the crosslinked structure. Network rearrangement allows vitrimers to relax stress and change shape. Conventional thermosets generally provide good mechanical strength and chemical resistance but their permanent structure makes them difficult to repair or reprocess after curing. Vitrimers keeps crosslinked thermoset structure but can still be reshaped or reprocessed when bond exchange is activated. [1][2]

CANs can be divided into associative and dissociative networks according to how their dynamic bonds rearrange. In an associative exchange, a new covalent bond is formed before or at the same time as the original bond is broken. The number of crosslinks therefore remains nearly constant during the rearrangement. Vitrimers were originally defined according to this associative behaviour. Dissociative CANs follow a different route. An existing bond first breaks and later it replaced by a new one, causing a temporary decrease in crosslink density. This difference affects the way the material flows and responds to heat. Associative networks usually maintain structure during the exchange process, while dissociative networks may show a more noticeable decrease in viscosity when the number of crosslinks is temporarily reduced.[1][2]

The performance of a vitrimer is closely related to the dynamic chemistry used in its network. Transesterification involves exchange reactions between ester and hydroxyl groups and is widely used in epoxy– and acrylate–based systems. It is also the most common mechanism among the vat–printable formulations examined in this thesis. Imine networks rearrange through reactions involving imine and amine groups, while disulfide systems rely on the exchange of S–S bonds. Boronic ester metathesis and vinylogous urethane exchange provide further routes for preparing repairable and reprocessable polymer networks. Each mechanism behaves differently depending on the network

composition. Some exchange reactions take place without a catalyst, whereas others require a catalyst, longer treatment, or higher temperature to reach a useful rate[1] [2][3].

Dynamic bonds does not indicate how quickly the network will rearrange by itself. Stress–relaxation tests are oftenly used to measure this behaviour. During the test, a fixed deformation is applied and the decrease in stress is followed over time. Faster relaxation at higher temperatures generally shows that the bond–exchange reactions are thermally activated. The glass–transition temperature and the temperature range in which the exchange reactions become sufficiently fast are also important. A vitrimer may remain stable under normal service conditions but become processable when it is heated to a temperature at which the network can rearrange within a practical time. These factors determine the conditions required for welding, repair, reshaping, and reprocessing.[1] [2]

The use of renewable materials adds another aspect to vitrimer design. Dynamic covalent bonds can support repair, reuse, and recycling, while bio–based raw materials can reduce dependence on fossil–derived feedstocks. Vegetable oils, lignin–derived aromatic compounds, glycerol, cellulose, sugars, and naturally occurring acids are among the main renewable resources used in vitrimer preparation. Their hydroxyl, carboxyl, epoxy, aldehyde, or unsaturated groups can be modified to produce monomers, crosslinkers, and reactive diluents. Agricultural and food–processing residues are also interesting because they can provide useful chemical building blocks from resources that might otherwise have limited value [3].

The term bio–based should still be used carefully. A resin may contain a renewable main component together with fossil–derived monomers, reactive diluents, catalysts, photoinitiators, or solvents. For this reason, the renewable content of the complete formulation should be considered rather than focusing on only one component. A bio–based origin also does not automatically make the cured network biodegradable. In the same way, renewable content alone cannot describe the overall environmental performance of a material. Processing energy, service life, repairability, recycling method, and end–of–life behaviour should be considered together. Combining renewable feedstocks with dynamic network chemistry can provide clear advantages, but the two aspects should not be treated as equivalent[4].

1.2 Processing and manufacturing methods of vitrimers

The manufacture of a vitrimer involves two parts. First, a permanently crosslinked network must be formed. The dynamic bonds within that network are then activated during repair, reshaping, or reprocessing. Many thermally cured vitrimers are prepared by mixing a resin with a crosslinker and when needed a catalyst. The mixture is cast into a mould and heated until curing is complete. Once the network has formed, further heating increases the bond–exchange rate and allows the material to be reshaped under pressure. Early epoxy vitrimer systems showed that crosslinked materials could be joined and shaped through heating without being converted into soluble polymers. The same principle was later used in hot pressing, grinding and remoulding, compression moulding, and repeated reprocessing[1][2].

These conventional methods are effective, but the initial shape usually depends on a mould or forming tool. Additive manufacturing offers more freedom because a part can be produced directly from a digital model. Vat photopolymerization is particularly suitable for liquid photocurable formulations and can produce complex geometries with good surface quality. Before printing, the three–dimensional model is divided into thin digital layers. Selected regions of the liquid resin are exposed to light and converted into a solid polymer. Once a layer has formed, the platform moves and fresh resin covers the printing area before the next exposure[5] [6], [7].

Stereolithography (SLA), digital light processing (DLP), and LCD–based printing use this general layer–by–layer principle, but they deliver light in different ways. SLA normally uses a laser that scans the required area point by point. A DLP printer projects the image of a complete layer using a digital micromirror device. In LCD printing, a liquid crystal screen acts as a mask and controls which regions of the resin receive light. DLP and LCD can expose many points within a layer at the same time, while SLA produces the image through the movement of a laser. These differences affect printing speed, exposure control, resolution, and the selection of suitable resin formulations[6], [7].

A typical vat–printing resin contains photocurable monomers or oligomers together with a photoinitiator. The photoinitiator absorbs light within a suitable wavelength range and produces the reactive species that begin polymerization. Acrylate and methacrylate groups are frequently used because they can polymerize rapidly through a radical mechanism and form a crosslinked network under UV or visible light. Other photopolymerization routes

are also possible, but the resin chemistry and photoinitiator must remain compatible with the wavelength and intensity provided by the printer [5], [6].

Rapid polymerization alone does not guarantee successful printing. The uncured resin must flow easily enough to cover the printing area after each layer, while the exposed resin must cure deeply enough to create strong bonding between layers. Over light penetration can cure resin outside the intended region and reduce dimensional accuracy. If penetration is insufficient, the layers may be weak or the part may fail during printing. Exposure time, light intensity, layer thickness, viscosity, and curing depth are therefore closely connected. Reactive diluents can reduce viscosity and improve resin flow, while light absorbers can limit excessive curing and help preserve small features[5], [6], [7].

Further difficulties can appear when fillers are added. A filler may increase mechanical strength or introduce thermal, electrical, or magnetic functions but it may also increase viscosity and scatter or absorb the printing light. Its concentration and dispersion must be controlled so that the additional function does not prevent reliable curing. This balance becomes more demanding in printable vitrimer systems. The resin must first polymerize rapidly enough to form an accurate part, while the dynamic bonds must remain available for later repair, welding, reshaping, or reprocessing. The final formulation is therefore determined by the combined effects of resin flow, photocuring behaviour, network stability, and bond–exchange rate[6].

Chapter 2: Bio–based vitrimer formulations

In this chapter, a formulation is considered vat–photopolymerized only when the source reports the production of three–dimensional objects by DLP, LCD/MSLA, or another vat–based process. A photocured film or test specimen alone is not treated as proof of 3D printing. The first part of the chapter therefore covers systems with direct vat–printing evidence. The second part presents bio–based vitrimer networks that were prepared by thermal curing, casting, or conventional photopolymerization but have not yet been demonstrated in vat printing. These non–printed systems are included because their exchange chemistry and material properties may guide the design of future printable resins.

2.1 3D Printed bio–based vitrimer formulations

2.1.1 Transesterification

Transesterification is the most widely studied exchange mechanism among the systems reviewed. Its fundamental mechanism involves the dynamic exchange between an ester group and a free hydroxyl group. Using different materials that have hydroxyl and ester groups also makes transesterification possible. Changing the molecular structure of these groups directly affects the material's physical properties and mechanical performance. Above the topological freezing temperature (*Tv*), these bonds are continuously broken and reformed. In some cases, in addition to the presence of hydroxyl and ester bonds, visible light is used to create parts to be printed into the desired shape, just like traditional thermosets. After printing, heating above Tv activates ester–hydroxyl exchange and allows the network to rearrange. Studies have shown that polymers subjected to thermal treatment above *Tv* following 3D printing shows superior mechanical strength and performance compared to those cured solely by light, as the polymer network is fully completed and internal stresses are effectively relaxed.[8]

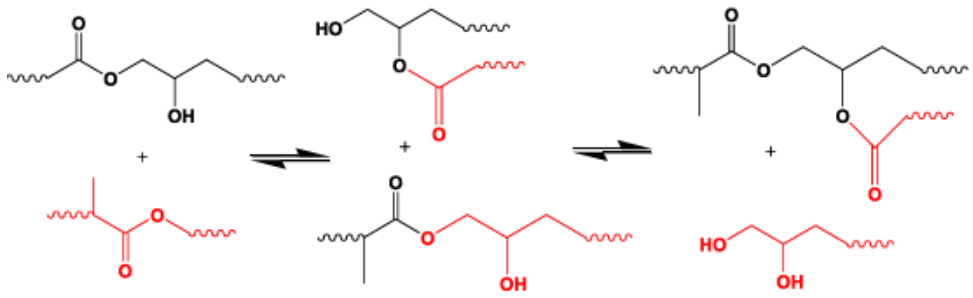


Figure 1 – The mechanism of the transesterification[8]

2.1.1.1 GDGDA–THFMA

The GDGDA–THFMA system was developed as a simple DLP–printable vitrimer based on two commercially available monomers with renewable origins. Glycerol 1,3–diglycerolate diacrylate (GDGDA) provides acrylate groups for photocuring and also contains the ester and hydroxyl groups needed for transesterification. Its main limitation is its high viscosity. Tetrahydrofurfuryl methacrylate (THFMA), which can be produced from furfuryl alcohol, was therefore used as a reactive diluent. It lowers the viscosity, takes part in the photocuring reaction, and introduces a relatively rigid ring structure into the network. TPO–L was used to initiate radical photopolymerization, while Miramer A99 was added to promote transesterification[8].

Several GDGDA/THFMA ratios were compared before printing. The formulation containing 60 wt% GDGDA and 40 wt% THFMA gave the best performance. It reached a double–bond conversion of about 92%, had a viscosity of 1394 mPa·s, and formed a gel within 2 s under the test conditions. These values were suitable for DLP processing, and three–dimensional objects with good structural definition were obtained. The printed network also showed temperature–dependent stress relaxation. The time required to reach the 1/e modulus level decreased from about 5.5 h at 180 °C to 2.3 h at 220 °C[8]. And the mixture also showed remarkable values in tensile test after welding.

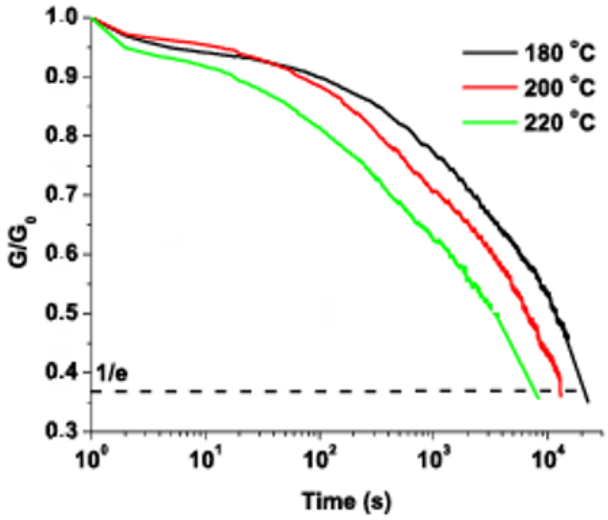


Figure 2 – Stress relaxation curve of GDGDA–THFMA[8]

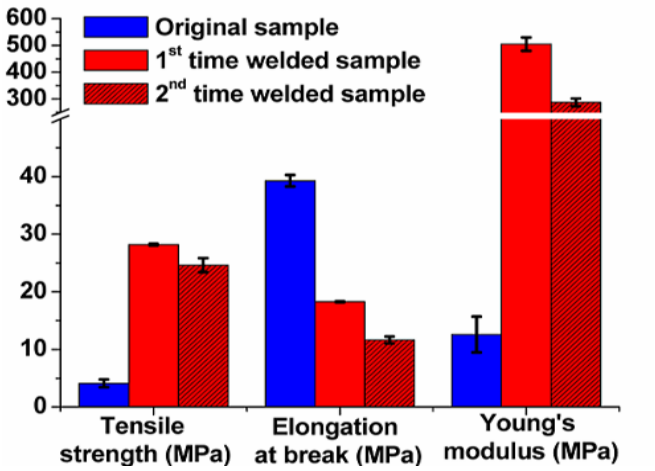


Figure 3 – Mechanical properties of GDGDA–THFMA[8]

2.1.1.2 DGEVADMA–HPPA

Vanillin–derived difunctional methacrylate, DGEVA dimethacrylate (DGEVADMA), with 2–hydroxy–2–phenoxypropyl acrylate (HPPA) used for creating vitrimer mechanism in this work. DGEVADMA acts as the main crosslinker and increases network rigidity. HPPA is

monofunctional and has a lower viscosity, so it improves resin flow and helps the formulation spread into a uniform layer during vat printing. HPPA also contains both hydroxyl and ester groups, which support transesterification after the photocured network has formed. TPO–L was used as the radical photoinitiator, and zinc acetylacetonate, $Zn(acac)_2$, was added as the transesterification catalyst[9].

The formulation selected for DLP printing contained 20 wt% DGEVADMA and 80 wt% HPPA, together with 3 mol% TPO–L and 5 mol% $Zn(acac)_2$. The high HPPA content kept the viscosity within a printable range, while the difunctional vanillin–based monomer provided enough crosslinking to maintain the shape of the printed parts. The resin was processed using 405 nm light and 50 µm layers[9]. The printed specimens showed stress relaxation that became much faster as the temperature increased, which is consistent with a catalyst–assisted transesterification mechanism.

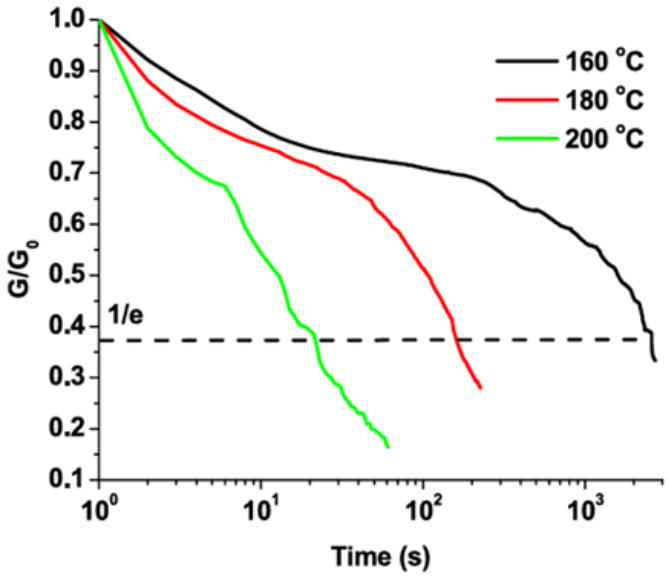


Figure 4 – Stress relaxation curve of DGEVADMA–HPPA[9]

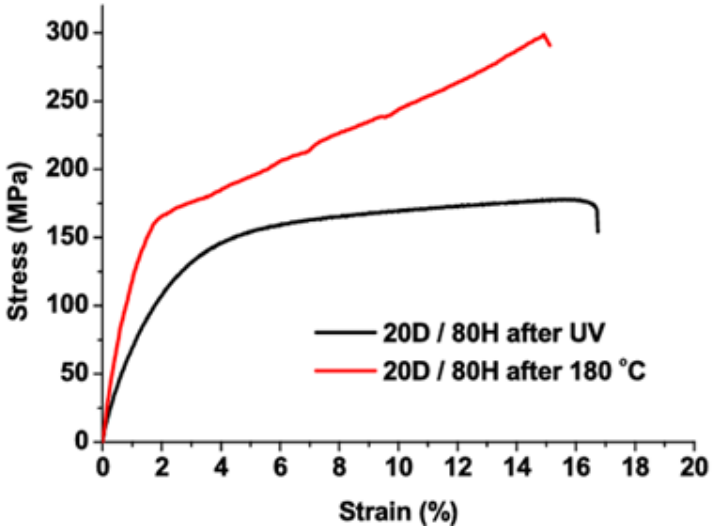


Figure 5 – Stress–strain graph of DGEVADMA–HPPA[9]

The material was examined for welding, shape memory, and chemical recycling. Heated interfaces recovered a high level of strength; in the reported test, the welded specimen reached a tensile–strength efficiency above 100%, most likely because heating also completed further curing and improved the network near the joint. This study is important because it links a vanillin–derived crosslinker with practical DLP processing and several vitrimer functions. At the same time, the formulation is only partly bio–based, since HPPA, the catalyst, and the photoinitiator should not be assumed to come from renewable sources[9].

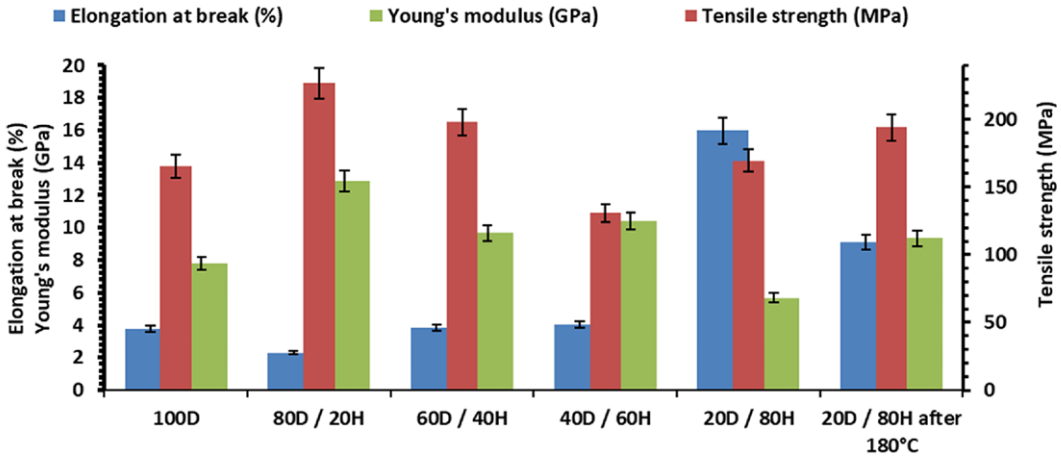


Figure 6 – Mechanical properties of DGEVADMA–HPPA[9]

2.1.1.3 HPPA–MCC

The HC10 formulation uses cellulose recovered from Aloe vera peel waste as a renewable crosslinking component. The extracted microcrystalline cellulose was methacrylated and becames Methacrylate microcrystalline cellulose (MCC) so that it could participate in radical photocuring. This modification is essential because unmodified cellulose does not readily form a covalent network with acrylate resins under vat–printing conditions. HPPA (2–hydroxy–3–phenoxypropyl acrylate) served as the main liquid monomer and supplied ester and hydroxyl groups for transesterification. Miramer A99 promoted the exchange reaction, and BAPO was used as the photoinitiator.[10]

The selected HC10 resin contained 75 wt% HPPA, 10 wt% MCC, and 15 wt% Miramer A99, with 2 phr BAPO. A higher cellulose content caused aggregation and less suitable flow behaviour[10], while the 10 wt% level gave a better balance between renewable content, dispersion, and printability.

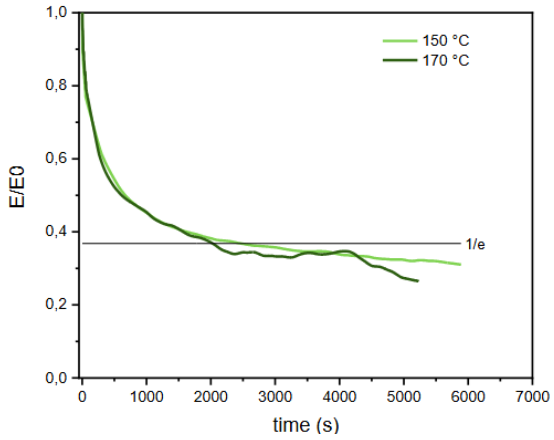


Figure 7 – Stress relaxation curve of HC10[10]

Stress–relaxation tests between 150 and 170 °C confirmed a heat–activated dynamic response, and the material reached the 1/e before 30 min. Heat treatment also changed the mechanical behaviour strongly. After treatment at 180 °C for 24 h, the elastic modulus increased from 43 MPa to about 1815 MPa, while elongation decreased from about 160% to 4%[10]. This means that the treatment produced a stiffer and less flexible network, rather than simply improving every property. The material could also be repaired and reshaped by heating. HC10 is also useful example of agricultural waste being converted into a functional component of a DLP–printable vitrimer, but its strong post–treatment stiffening must be considered when selecting an application.

2.1.1.4 AESO–AEUG–EUGP

AESO–AEUG–EUGP was designed for bioactive scaffolds and combines a renewable vitrimer matrix with inorganic particles. Acrylated epoxidized soybean oil (AESO) is the main resin and provides a multifunctional structure for photocuring. Acrylated eugenol (AEUG) acts as a lower–viscosity reactive component and also increases the renewable fraction of the formulation. A eugenol–derived phosphate ester (EUGP), was used as the transesterification catalyst. The unfilled matrix contained AESO and AEUG at a 70:30 ratio, with 10 phr EUGP and 2 phr photoinitiator[11].

Later, 30 phr tellurium–doped bioactive glass (BG–Te) or a silanized form of the same glass (BG–Te–Sil) added to formulation. The silane treatment introduced methacrylate groups intended to improve bonding between the particles and the polymer network. The fillers also affected photocuring. After 2 min of irradiation, double–bond conversion was about 86% for the unfilled resin, 80% for the BG–Te formulation, and 54% for BG–Te–Sil. This reduction shows a practical limitation of filled vat resins: particles can absorb or scatter light and reduce curing efficiency[11]. The resin was still used to print scaffold geometries by DLP, and stress–relaxation measurements at 180 °C showed that the printed network retained vitrimer behaviour.

The main benefit of the glass was not limited to mechanical reinforcement. The study examined biological response and bacterial adhesion because the target use was hard–tissue engineering. The BG–Te surface reduced Staphylococcus aureus (Gram–positive bacterium) adhesion by 87% compared with the unfilled matrix and by 54% compared with BG–Te–Sil. The materials also supported attachment and growth of human bone–marrow–derived mesenchymal stem cells. The work therefore shows how a bio–based printable vitrimer can be given bioactive and antibacterial functions. It also shows that filler surface treatment does not automatically improve every property, since BG–Te–Sil produced the lowest photocuring conversion in this formulation[11].

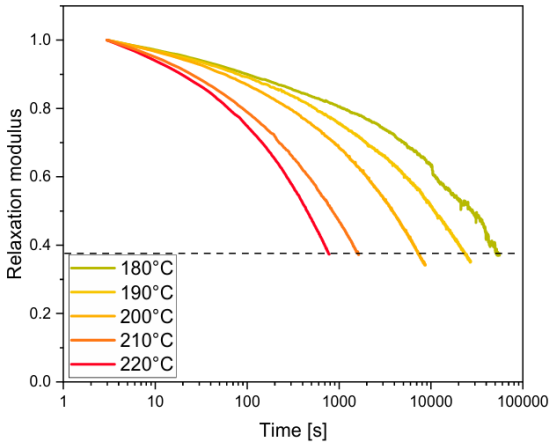


Figure 8 – Stress–relaxation graph of AESO–AEUG–EUGP with BG–Te[11]

2.1.1.5 THFMA–AESO–HPPA

The THFMA–AESO–HPPA resin was used to improve the balance between viscosity, renewable content, photocuring, and vitrimer response. 2–hydroxy–3–phenoxypropyl acrylate (HPPA) was used as the main source of ester and hydroxyl groups for transesterification. Acrylated epoxidized soybean oil (AESO) introduced a renewable multifunctional component and increased network flexibility. Tetrahydrofurfuryl methacrylate (THFMA) acted as a reactive diluent. It lowered the viscosity and became part of the network during light curing, so no non–reactive solvent was needed. TPO–L initiated radical photopolymerization, while Miramer A99 promoted the later transesterification reaction.[12]

The selected formulation contained 50 wt% HPPA, 40 wt% THFMA, and 10 wt% AESO, together with 3 mol% TPO–L and 5 wt% Miramer A99. Its viscosity was 413 mPa·s, which is suitable for a vat system. The degree of double–bond conversion was 73.8%, and the gel time was 12 s under the reported test conditions. DLP printing was successfully demonstrated in this work and the material had a glass–transition temperature near 7 °C and a topological freezing temperature of about 66 °C. Stress relaxation became faster with increasing temperature, with the reported 1/e time decreasing from 145 min at 160 °C to 16 min at 220 °C.[12]

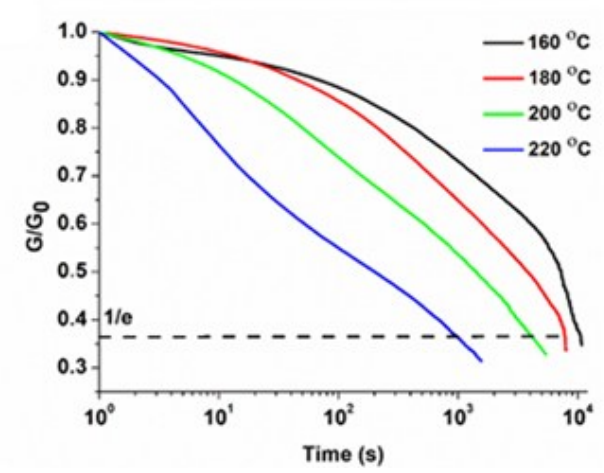


Figure 9 – Stress–relaxation graph of THFMA–AESO–HPPA [12]

Heating also enabled repair and reprocessing. Low initial stiffness was expected from the high fraction of monofunctional components and the flexible soybean–oil segment. The initial tensile test value was aroıund 0.27 MPa[12]. After welding for 4 h at 180 °C, the tensile strength increased two times and Young's modulus increased six times of the original. So, the formulation demonstrates that a small amount of AESO can be combined with two low–viscosity monomers to produce a DLP–printable vitrimer with a clear thermal exchange response. Its main trade–off is that the flexible and dilute network provides easy processing but low initial mechanical strength.

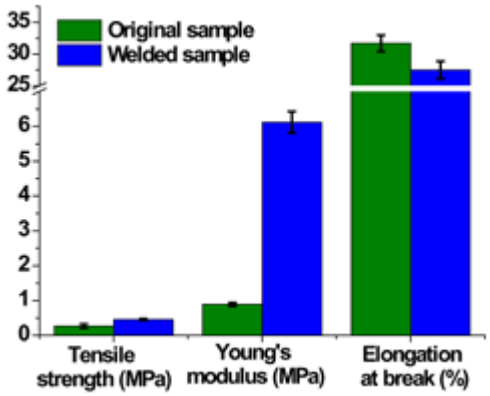


Figure 10 – Mechanical properties of THFMA–AESO–HPPA [12]

2.1.1.6 DPEPA–GDGDA–GLYFOMA–RTE

The N5 formulation was designed as a catalyst–free, rapidly photocurable vitrimer resin for LCD printing. It contained four reactive components: dipentaerythritol penta–/hexa–acrylate (DPEPA), 1,3–diglycerolate diacrylate (GDGDA), glyceryl formal methacrylate (GLYFOMA), and resveratrol triglycidyl ether (RTE). DPEPA and GDGDA increased functionality and helped the resin form a rigid network. GLYFOMA reduced viscosity, while RTE introduced an epoxy component and helped limit polymerization shrinkage. The feedstocks have different renewable links: DPEPA can be prepared from modified

vegetable–oil chemistry, GDGDA and GLYFOMA are related to glycerol, and RTE is derived from resveratrol[13].

N5 contained 30 wt% DPEPA, 30 wt% GDGDA, 30 wt% GLYFOMA, and 10 wt% RTE. The additives were 2.5 wt% TPO, 2 wt% CPI–410S, and 0.08 wt% UVB. TPO is a radical photoinitiator and CPI–410S is a cationic photoinitiator. UVB was used to control light penetration and did not act as a third photoinitiator. The formulation had a viscosity of 381 mPa·s and a gel time of 1.75 s and it was printed with an LCD printer at 405 nm[13].

The cured material was thermally stable, with 5% mass loss at about 402 °C. When the mechanical properties are inspected, it showed a Young's modulus of 767 MPa and a tensile strength of 16 MPa. Its elongation at break was only about 0.2%, so the network was very brittle. The material showed transesterification–based relaxation without an added exchange catalyst, and its topological freezing temperature was reported as 108 °C[13]. Welding and repeated reprocessing were possible, but the mechanical properties decreased. After welding, tensile strength fell from 16 to 7 MPa, and repeated cycles caused further loss. N5 is therefore a strong example of fast printing and high thermal stability, but it also shows that reprocessability alone does not guarantee complete recovery of mechanical performance.

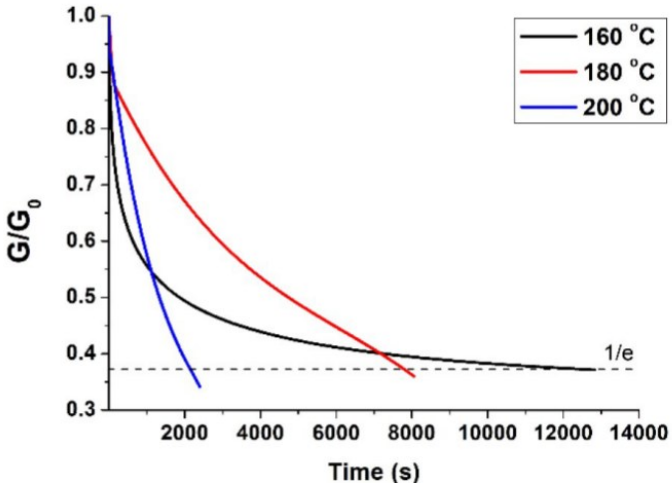


Figure 11 – Stress relaxation curve of DPEPA–GDGDA–GLYFOMA–RTE [13]

2.1.1.7 HPPA–AESO

The HPPA–AESO system uses 2–hydroxy–2–phenoxypropyl acrylate (HPPA) as the main low–viscosity monomer and acrylated epoxidized soybean oil (AESO) as a renewable multifunctional crosslinker. HPPA supplies ester and hydroxyl groups for transesterification and also improves resin flow. AESO increases the number of photocurable groups and introduces flexible fatty–acid segments. Zinc acetylacetonate was used to catalyse bond exchange, and TPO–L was used for photopolymerization. Several ratios were studied to determine how the AESO content affected viscosity, curing, and mechanical behaviour [14].

The formulation selected for DLP printing contained 90 wt% HPPA and 10 wt% AESO, with 5 mol% $Zn(acac)_2$ and 3 mol% TPO–L. This composition remained fluid enough for vat processing while forming a stable crosslinked object. The printed material showed a topological freezing temperature of about 72 °C and clear temperature–dependent stress relaxation[14]. Also shape memory, repair, reprocessing, welding, and alcoholysis are demonstrated. Shape recovery reached 100% in the reported test. The measured self–healing was 47% and reprocessing efficiencies was 31% and which gives a more realistic view of the limits of the system.

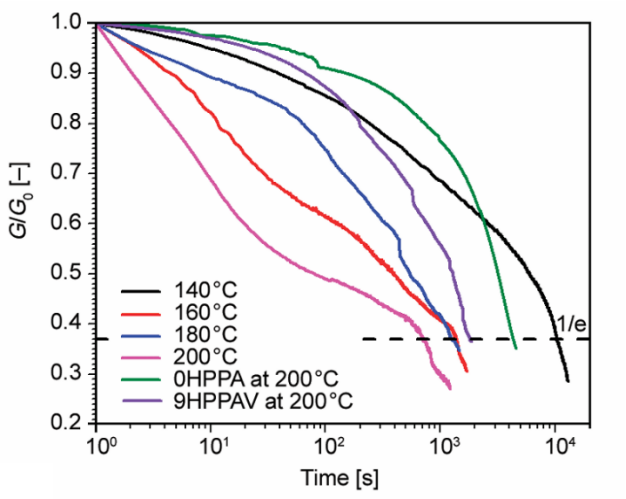


Figure 12 – Stress–relaxation graph of *HPPA–AESO. The values for 140 °C, 160 °C, 180 °C, 200 °C indicates the formulation 90 wt% HPPA and 10 wt% AESO. 0HPPA represents 100 wt% AESO and 9HPPAV represents post cured vitrimer at 200 °C for 4 h.* [14]

A tensile strength of 1.39 MPa was measured and in the self–healing test, the parts joined within 1 h at 200 °C, and the self–healing efficiency was recorded as 47%.[14]

	HPPA/AESO	HPPA/AESO/THFMA
Ratio	90% HPPA, 10% AESO	50% HPPA, 10% AESO, 40% THFMA
Catalyst	5 mol% $Zn(acac)_2$	5 wt% Miramer A99
Gel point	2 s	12 s
G′	23.25±1.55 MPa	57.19 MPa
Stress relaxation at 200 °C	11.5 min	~ 66 min
Tensile strength	1.39 MPa	~ 0.27 MPa
Elongation at break	80.47%	~ 31%

Table 1 – Comparison of HPPA–AESO and HPPA–AESO–THFMA [12]

2.1.1.8 AERO–HPPA–GDGDA

This formulation family uses acrylated epoxidized rapeseed oil (AERO), 2-hydroxy-3-phenoxypropyl acrylate (HPPA), and glycerol 1,3–diglycerolate diacrylate (GDGDA). AERO adds a renewable, flexible, multifunctional component. HPPA lowers viscosity and provides hydroxyl and ester groups for transesterification. GDGDA increases crosslink density and stiffness because it has two acrylate groups. Three monomer ratios were compared with formulation name AERO10 and contained 10 wt% AERO, 70 wt% HPPA, and 20 wt% GDGDA; AERO20 contained 20/70/10 wt%; and AERO30 contained 30/70/0 wt%. Catalysed and catalyst–free versions were prepared, and TPO–L was used for photocuring.[15]

AERO30 had the highest rapeseed–oil content and the lowest viscosity, about 663 mPa·s, because it did not contain GDGDA. It was selected for DLP printing and produced parts with a smooth surface and good dimensional definition at 50 µm layer thickness. The comparison with and without $Zn(acac)_2$ showed that the catalyst strongly accelerated stress relaxation. At 200 °C, the catalysed formulations reached the 1/e level in about 10–16 min, while the catalyst–free versions required roughly 31–34 min. The catalyst was therefore

useful for exchange, although its effect on light curing and network formation also had to be considered.

Resins	Ratios
AERO10	10% AERO, 70% HPPA, 20% GDGDA
AERO20	20% AERO, 70% HPPA, 10% GDGDA
AERO30	30% AERO, 70% HPPA

Table 2 – Formulations of AERO–HPPA–GDGDA [15]

Hot–press reprocessing at 200 °C 2 h was applied for two cycles[15]. Catalysed samples formed more uniform recycled sheets, while visible cracks remained in some catalyst–free samples. The printed formulation was also repaired by heat treatment, and the repaired specimens could show higher tensile properties than the original printed parts most possible cause is heating led to bond exchange and additional network development. The formulation data show a clear compromise: GDGDA increased rigidity, whereas increasing the AERO content lowered viscosity and raised the renewable fraction but produced a softer network. The work also shows that transesterification can occur without an added catalyst, although more severe or longer thermal treatment is then required

Resins	Relaxation time with catalyst 200 °C	Relaxation time without catalyst 200 °C
AERO10	10 min	31 min
AERO20	16 min	34 min
AERO30	14 min	33 min

Table 3 – Stress relaxation table of AERO–HPPA–GDGDA with and without catalyst [15]

2.1.1.9 AELO–EGMP–TMP3MP–DMEP

This study used acrylated epoxidized linseed oil (AELO) as the main renewable resin. The network was formed by a thiol–acrylate photoreaction using either ethylene glycol bis–mercaptopropionate (EGMP) or trimethylolpropane tris(3–mercaptopropionate)

(TMP3MP). The thiol compounds change the network functionality and therefore affect viscosity, stiffness, and the speed of transesterification. Bis(2–methacryloyloxy ethyl) phosphate (DMEP) was used as the transesterification catalyst, BAPO as the photoinitiator, and a small amount of Sudan II as a light absorber to control the curing depth.[16]

The AELO–EGMP resin was much less viscous than the AELO–TMP3MP resin, with reported viscosities of about 2.1 and 11.9 Pa·s, respectively. The lower viscosity made AELO–EGMP more suitable for DLP printing. It also relaxed stress more quickly. At 180 °C, the catalysed AELO–EGMP network reached 63% stress relaxation in 22 min, while the same network without catalyst required 384 min[16]. The AELO–TMP3MP network needed about 77 min under comparable conditions. The cause of relaxation time difference of the samples attributed to the higher crosslinking degree of the AELO–TMP3MP.

Properties	AELO–EGMP	AELO–TMP3MP
Viscosity	2.1 Pa·s	11.9 Pa·s
Acrylate conversion	97%	87%
Thiol conversion	48%	46%
Gel content	~71%	~77%
Relaxation at 180 °C	22 min	77 min
Tensile strength	0.58 MPa	1.18 MPa

Table 4 – Comparison of AELO–EGMP and AELO–TMP3MP [16]

The printing formulation contained 70 wt% AELO, 20 wt% EGMP or TMP3MP, 8 wt% DMEP, and 2 wt% BAPO, with 0.05 wt% Sudan II. DLP printing produced structures with features around 550 μm and with 405 nm light source. The printed objects could be reshaped and healed by heating, and thermal treatment improved their toughness. However, the mechanical strength remained moderate; the AELO–EGMP and AELO–TMP3MP networks had tensile strengths of about 0.58 and 1.18 MPa[16]. The formulation is therefore more suitable for flexible or low–load applications than for highly structural parts. Its main impact is the application of a highly renewable linseed–oil resin that can be printed and later repaired through transesterification.

2.1.2 Imine bonds

Imine bonds are dynamic covalent bonds commonly formed through a condensation reaction between a primary amine and an aldehyde or ketone, usually seen with the release of water. Under suitable conditions, imine formation is reversible, which allows these bonds to be used as dynamic crosslinking points in vitrimer networks. Heating generally increases the rate of bond exchange and improves network mobility, enabling properties such as self–healing, welding, reshaping, and thermal reprocessing[3].

Imine network rearrangement can occur through transimination, imine metathesis, or hydrolysis followed by imine reformation. Transimination involves the reaction of an existing imine bond with a free primary amine, resulting in the formation of a new imine bond. Imine metathesis involves the exchange of groups between existing imine bonds without requiring free amine groups. The dominant mechanism depends on the network composition and reaction conditions[3].

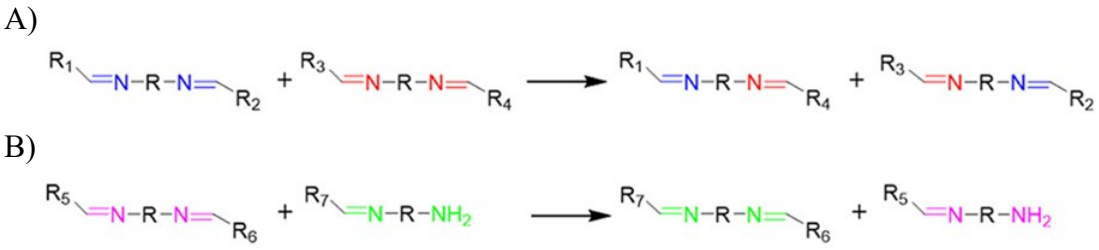


Figure 13 – A)Transimination B)Imine methathesis [17]

2.1.2.1 HMDA–MAV–EGPMA

In this system, vanillin was first converted into vanillin methacrylate (MAV). Two MAV molecules were then reacted with hexamethylenediamine (HMDA) to produce HMDA–MAV, a difunctional crosslinker containing two methacrylate groups and two imine bonds. The methacrylate groups enable network formation through radical photopolymerization, while the imine bonds provide the dynamic exchange mechanism. Ethylene glycol phenyl ether methacrylate (EGPMA) was used as a monofunctional reactive diluent to reduce the

crosslink density, improve flexibility, and obtain a viscosity suitable for processing. TPO was used as the photoinitiator. The renewable contribution of the formulation mainly comes from vanillin, while HMDA and EGPMA should not be considered bio–based without further evidence[18].

The sample names directly indicate their composition and curing method. “UV” refers to photocuring, while the number represents the weight percentage of HMDA–MAV in the reactive resin mixture. Therefore, UV25 contained 25 wt% HMDA–MAV and 75 wt% EGPMA, whereas UV50 contained 50 wt% HMDA–MAV and 50 wt% EGPMA. Both formulations also contained 2 phr TPO, added relative to the total amount of resin. TPO was an additional component and was not included in the 100 wt% HMDA–MAV/EGPMA ratio[18].

Increasing the HMDA–MAV content increased the crosslink density, glass–transition temperature, and rubbery storage modulus. However, the room–temperature tensile properties of UV25 and UV50 remained similar. The higher concentration of imine bonds in UV50 resulted in faster stress relaxation. At 140 °C, UV25 and UV50 reached the 1/e relaxation level in 139 and 49 s, respectively. At 160 °C, these times decreased to 52 and 34 s. Different photoinitiators are also compared and observed faster relaxation in samples containing TPO or BAPO, suggesting that phosphine oxide groups assisted imine metathesis. In the results, UV50 at 140 °C, showed relaxation in 49 s with TPO and 37 s BAPO. This result shows the effect of photoinitiators in relaxation behaviour. [18]

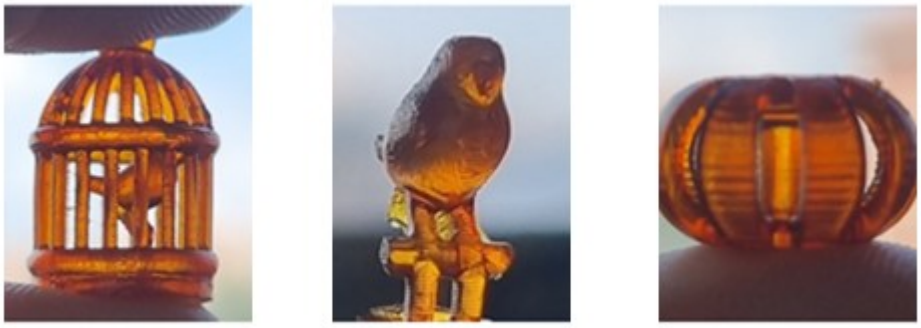


Figure 14 – 3D printings of UV25 resin system [18]

UV25 was selected for DLP printing and was successfully used to produce complex objects with a Z–direction resolution of 100 μm. The damaged surface of UV25 was completely repaired after heating at 160 °C for 1 h[18]. Mechanical recycling was also demonstrated by grinding and hot–pressing the material. It shows that this study presents a partly bio–based, DLP–printable polyimine vitrimer with rapid stress relaxation, thermal repair, and reprocessing ability.

2.1.2.2 CROSS–BDG–IBOMA

The CROSS–BDG–IBOMA system was built from vanillin–derived imine molecules with different functionalities. CROSS is a trifunctional, photocrosslinkable imine compound produced from 2–(Methacryloyloxy) ethyl vanillin (MEV) and tris(2–aminoethyl)amine (TREN). BDG is a bifunctional imine building block prepared using a fatty–acid–derived Priamine and MEV. Isobornyl methacrylate (IBOMA), a rigid reactive diluent related to terpene feedstocks, was added at 20 wt% to reduce viscosity and improve vat processing. BAPO was used as the photoinitiator. By changing the ratio of CROSS and BDG, crosslink density could adjust without removing the dynamic imine chemistry[19].

Formulation	CROSS (wt%)	BDG (wt%)	IBOMA (wt%)	Biobased content (wt%)
CROSS – 0	0	80	20	75
CROSS – 5	5	75	20	74
CROSS – 10	10	70	20	73

Table 5 – Different formulations of CROSS–BDG–IBOMA resin [19]

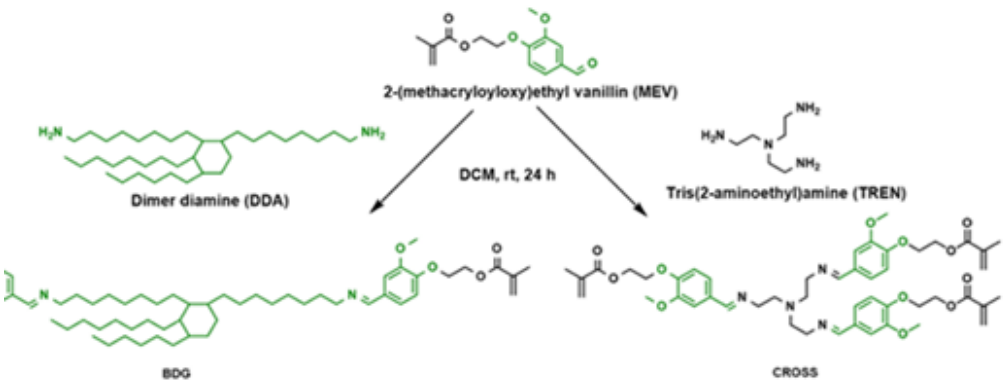


Figure 15 – Reaction scheme of BDG and CROSS [19]

A higher CROSS content produced a stiffer material and increased the number of exchangeable imine bonds in the network. This also supported faster stress relaxation. A higher BDG content introduced longer, more flexible segments and reduced stiffness. The addition of IBOMA was important for printing because the original imine building blocks were too viscous for easy recoating. After the viscosity was adjusted, high–resolution objects with complex shapes were produced by DLP. The printed parts were thermally stable and retained a rigid character at room temperature.

Mechanical recycling was demonstrated by grinding the cured material and hot–pressing it at 150 °C under 40 kN for 5 min[19]. The procedure was repeated for three cycles. The short processing time shows the benefit of rapid imine exchange, although repeated recycling still needs to be evaluated in terms of full property retention and ageing. This formulation is a strong example of molecular design: a trifunctional unit provides structural strength, a bifunctional fatty segment controls flexibility, and IBOMA brings the viscosity into a printable range. Several components have renewable origins, but the exact bio–based fraction depends on the chosen CROSS/BDG ratio and on the source of the commercial reagents.

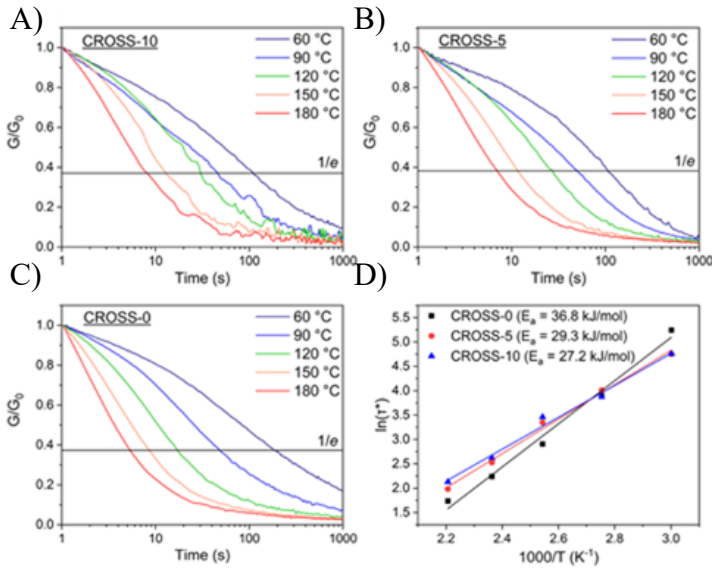


Figure 16 – A) Stress relaxation curve of CROSS–10 B) Stress relaxation curve of CROSS–5 C) Stress relaxation curve of CROSS–0 D) Activation energy of CROSS–0, CROSS–5 and CROSS–10 [19]

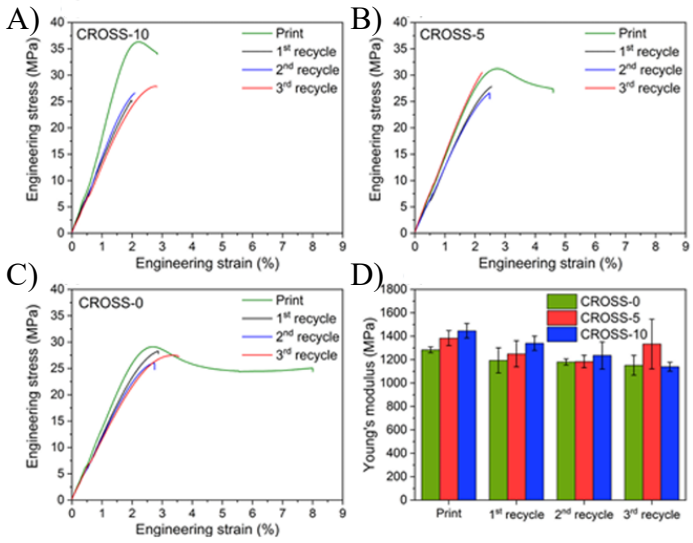


Figure 17 – A) Stress–strain graph of CROSS–10 B) Stress–strain graph of CROSS–5 C) Stress–strain graph of CROSS–0 D) Young's modulus of CROSS–0, CROSS–5 and CROSS–10 according to cycles [19]

2.1.3 Disulfide bonds

Disulfide bonds are dynamic S–S bonds formed between two sulfur atoms[3]. These bonds are generally produced through the oxidation of two thiol groups (–SH). The formation and exchange behavior of disulfide bonds are affected by environmental conditions such as temperature and pH. High temperature facilitates the cleavage and rearrangement of S–S bonds.

During heating, reversible bond exchange occurs between disulfide bonds. This process is referred to as disulfide metathesis or disulfide exchange. During the exchange, the bonding partners of the S–S bonds within the network change. Consequently, the polymer–network topology can be rearranged without completely eliminating the crosslinked structure.

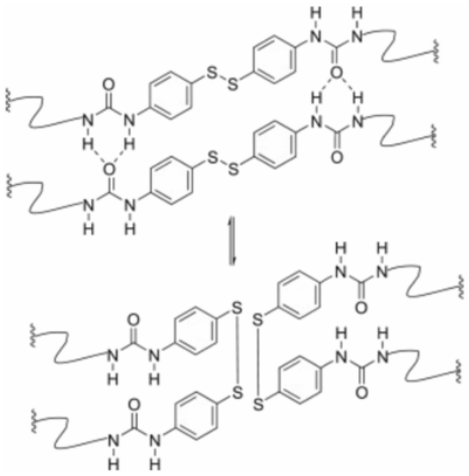


Figure 18 – Disulfide bonds exchange mechanism [20]

The disulfide–exchange mechanism can provide stress relaxation with a relatively low activation energy. This property allows the material to dissipate energy under stress and reduce damage formation. The ability of the network to rearrange also enables disulfide–based vitrimers to exhibit self–healing, welding, reshaping, and thermal–reprocessing properties.

In some bio–based vitrimers, disulfide exchange is not used alone. Instead, it is combined with a second dynamic mechanism, such as transesterification or imine exchange, to form a dual–dynamic network. This approach can provide both rapid bond exchange and sufficient mechanical strength[3].

2.1.3.1 CMAV–IBA

CMAV is an imine and disulfide containing methacrylate crosslinker prepared from vanillin and cystamine. Its structure contains two imine bonds and one central disulfide bond, together with methacrylate groups for photopolymerization. Isobornyl acrylate (IBA) was used as a monofunctional reactive diluent. It lowers the viscosity, adds rigidity through its bicyclic structure and becomes part of the network during curing. TPO was used as the radical photoinitiator[21].

Three formulations were prepared with 15, 25, and 35 wt% CMAV, named R1, R2, and R3 accordingly. The remaining reactive component was mainly IBA, with 1.5 wt% TPO. Increasing the CMAV content increased crosslinker concentration and the number of dynamic bonds. The resins were processed by DLP, confirming that CMAV–IBA is a genuinely 3D–printed system rather than only a photocured film. The printed networks showed shape memory and self healing behaviour at room temperature and at 90 °C[21]. The combination of two exchange mechanisms was used to obtain rearrangement without removing the permanent crosslinked structure.

Resins	CMAV	IBA	TPO
R1	15%	83.5%	1.5%
R2	25%	73.5%	1.5%
R3	35%	63.5%	1.5%

Table 6 – Resin ratios of CMAV–IBA [21]

In this system, which was cured using 405 nm light, the tensile strengths of R1, R2, and R3 were 28.2, 31.4, and 32.6 MPa, respectively. After chemical recovery and reprinting, recycled R2 showed a tensile strength of 24.4 MPa and self healed R2 sample exhibited a

tensile strength of 27.4 MPa. The self healing behaviour mainly attributed to dynamic disulfide exchange, which can occur under mild conditions[21]. At room temperature, the cut pieces joined within 24 h, while complete healing required 8 d. Increasing the temperature accelerated the exchange process, and the crack was almost completely healed within 2 h at 90 °C.

2.2 Bio–based formulations not yet demonstrated by vat photopolymerization

The following systems show useful dynamic behaviour but were not printed by DLP, LCD/MSLA, or SLA in the cited studies. They were prepared by thermal curing, moulding, casting, hot pressing, or other laboratory methods. They are included as possible starting points for future resin design, not as existing vat–printable formulations. To become printable, each system would need suitable photocurable groups, a compatible photoinitiator, controlled viscosity, and enough light penetration to produce accurate layers.

2.2.1 Transesterification bonds without vat photopolymerization

2.2.1.1 FEP–FEHBP–CA

This fully bio–based epoxy vitrimer was prepared from ferulic acid derived epoxy resin (FEP), a ferulic acid based hyperbranched epoxy modifier (FEHBP), and citric acid (CA). FEP provides the main epoxy structure. CA opens the epoxy rings and forms ester bonds and hydroxyl groups, creating the chemical groups required for transesterification. FEHBP is a reactive part of the network rather than a separate filler. Its hyperbranched structure adds many epoxy and hydroxyl–containing sites and changes both crosslink density and chain mobility. Petroleum–based DGEBA was used only as a reference material in the study and should not be included in the name of the bio based formulation[22].

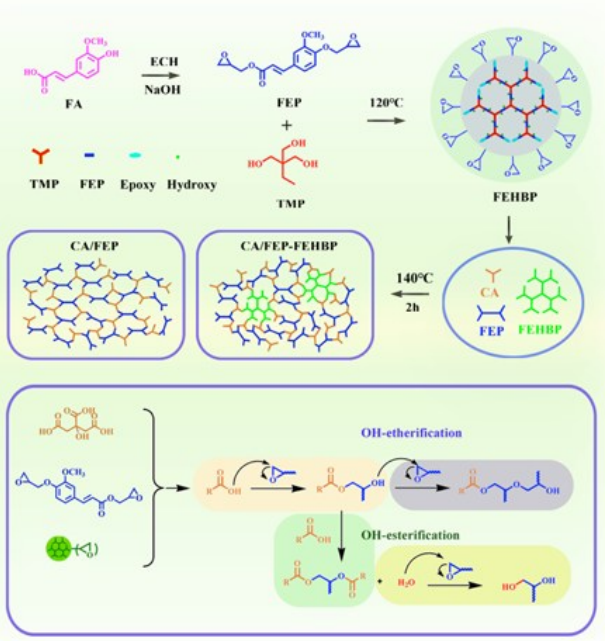


Figure 19 – Production of FEP and FEHBP and curing the vitrimer resin [22]

Adding 10 phr FEHBP gave the best performance. The modified network reached a tensile strength of 126MPa and relaxed stress rapidly at 140 °C, reaching the 1/e level in about 45 s[22]. The unmodified CA/FEP network required about 164 s under the same conditions. This result suggests that the hyperbranched modifier increased the number of accessible exchange sites while also improving strength. The material was reprocessed by cutting it into small pieces and hot–pressing at 140 °C under 5 MPa for 30 min. After repeated processing, more than 88% of the original tensile strength was retained.

Resins	Relaxation time at 140°C
CA/DGEBA	2745 s
CA/FEP	164 s
CA/FEP/FEHBP	45 s

Table 7 – Relaxation times of CA/DGEBA, CA/FEP, CA/FEP/FEHBP [22]

One of the most important features of this system is its closed–loop recyclability. Following alkaline depolymerization with NaOH, ferulic acid was recovered with a yield of 70.1%, while the citric–acid–derived component was obtained as a polyester oligomer (r–CAP), rather than as free citric acid. The system prepared again from the recycled materials exhibited a tensile strength of 121 MPa, shows its potential reuse with minimal loss of mechanical performance[22]

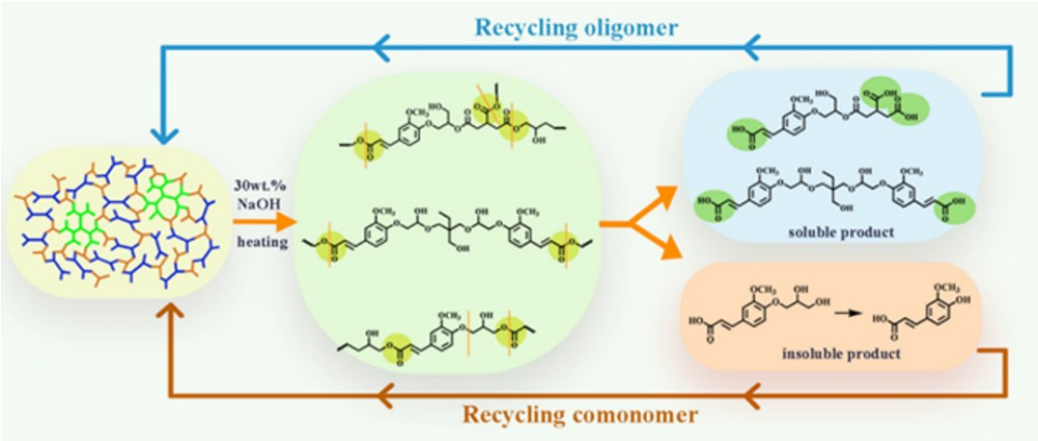


Figure 20 – Recycle scheme [22]

2.2.1.2 ESO–GL

The epoxidized soybean oil (ESO) and glycyrrhizic acid (GL) system was reported as a fully bio–based vitrimer as multifunctional compound obtained from licorice. The carboxylic–acid groups of glycyrrhizic acid react with the epoxy groups of ESO. This reaction forms ester bonds and free hydroxyl groups, which later support transesterification. Triazabicyclodecene (TBD) was used as the exchange catalyst. The study examined the effect of composition and catalyst content and selected a network with an carboxylic acid/epoxy ratio of 0.5 and 5 mol% TBD for detailed evaluation[23].

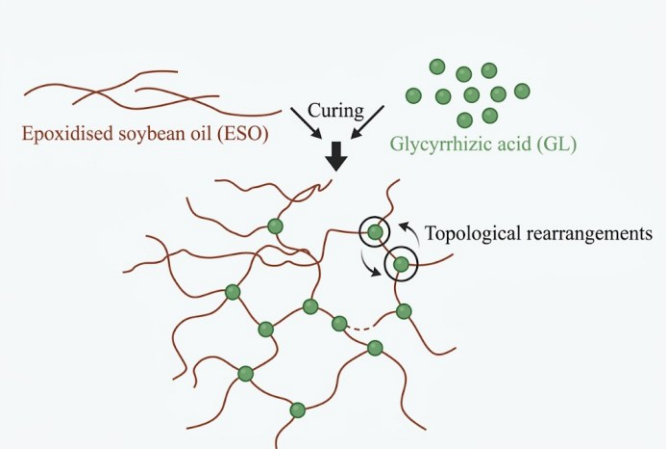


Figure 21 – Curing reaction of ESO and GL

The network showed temperature dependent stress relaxation, with a reported relaxation time in Table 9. Heating allowed the material to be welded, reshaped, and repaired. In lap–shear testing, the original, repaired and recycled specimens reached about 3.42, 2.89, and 2.49 MPa, respectively. These values show that useful adhesion and recovery were obtained, but they also show a gradual loss after repair and recycling. The material also showed shape–memory behaviour because the permanent network fixed the original shape while the dynamic exchange allowed rearrangement during heating.

Temperature	Relaxation time
140 °C	7.81 h
160 °C	1.14 h
180 °C	23 min
200 °C	7 min

Table 8 – Relaxation times of ESO–GL [23]

This formulation contains fully renewable materials and uses a simple epoxy–acid route, but it is not a vat printable resin in its reported form. The network was produced by thermal curing, and no photoinitiator or light reactive acrylate group was used. Its relaxation is also

slower than that of several imine and boronic ester based systems. Future use in vat photopolymerization would require a photocurable derivative of ESO or glycyrrhizic acid, together with viscosity control. The study remains relevant because it shows that soybean oil and a plant–derived multifunctional acid can produce a repairable covalent network without relying on a petroleum–based epoxy resin[23].

2.2.2 Imin bonds without vat photopolymerization

2.2.2.1 PV–1071 and PV–1074

PV–1071 and PV–1074 are vanillin–based polyimine networks prepared with two commercial bio–based polyamines, Priamine 1071 and Priamine 1074. Vanillin supplies the aldehyde groups, while the Priamine compounds provide primary amines and long aliphatic segments derived from fatty acids. Condensation between aldehyde and amine groups forms the imine crosslinks. The long fatty chains keep the network flexible enough for fast bond exchange, while the aromatic vanillin units contribute rigidity. The two Priamine grades have different amine structures, so they produce related but not identical network behaviour[24].

Both materials showed rapid stress relaxation between 80 and 120 °C, with the approximate values presented in Table 9 and could be reprocessed by hot pressing. Their reported activation energies were 12.33 kJ mol^{-1} for PV–1071 and 15.93 kJ mol^{-1} for PV–1074[24]. These low values are consistent with a fast imine exchange process. The networks also had tensile strengths around 5 MPa. Acid treatment broke the imine bonds and allowed the vanillin–derived aldehyde component to be recovered and reused. This gives the system both thermomechanical and chemical recycling routes.

Temperature	Relaxation time	
	PV–1071	PV⁻1074
80 °C	40 s	26 s
90 °C	34 s	24 s
100 °C	30 s	21 s
110 °C	27 s	19 s
120 °C	22 s	17 s

Table 9 – Approximate relaxation times of PV–1071 and PV–1074 [24]

The closed–loop chemical recycling properties of this imine–metathesis system were also investigated[24]. After degradation, PV separated from the solution as a solid and was recovered by filtration for reuse. The tests indicated a PV recovery of 69%, while the tensile strength and elongation values were close to those of the original system.

2.2.3 Disulfide bonds without vat photopolymerization

2.2.3.1 DGEVA–Cystamine

The DGEVA–Cystamine network is a bio–based epoxy vitrimer containing dynamic disulfide bonds. Diglycidyl ether of vanillyl alcohol (DGEVA) is a vanillin–derived diepoxy monomer. Cystamine is a diamine with a central disulfide bond. During curing, the amine groups open the epoxy rings and form a permanent crosslinked network, while the S–S bonds remain within the network strands and provide the dynamic exchange sites. The epoxy to amine functional–group ratio used for the main material was 1:1.2 [25].

At 140 °C, the original DGEVA–cystamine vitrimer showed complete stress relaxation with an average relaxation time of 74 s and an activation energy of 57 kJ mol^{-1}. For recycling, the vitrimer was crushed and combined with pure cystamine at 60 °C for approximately 24 h. Cystamine amounts equal to five and ten times the mass of the vitrimer resulted in complete depolymerization. The resulting mixtures were directly combined with DGEVA and cured again without solvent removal or purification. The recycled materials were

named DGEVA/cyst5(R) and DGEVA/cyst10(R), where 5 and 10 indicate the amount of cystamine used relative to the vitrimer mass and (R) indicates the recycled material. At 140 °C, DGEVA/cyst5(R) and DGEVA/cyst10(R) showed complete stress relaxation with average relaxation times of 367 s and 341 s.

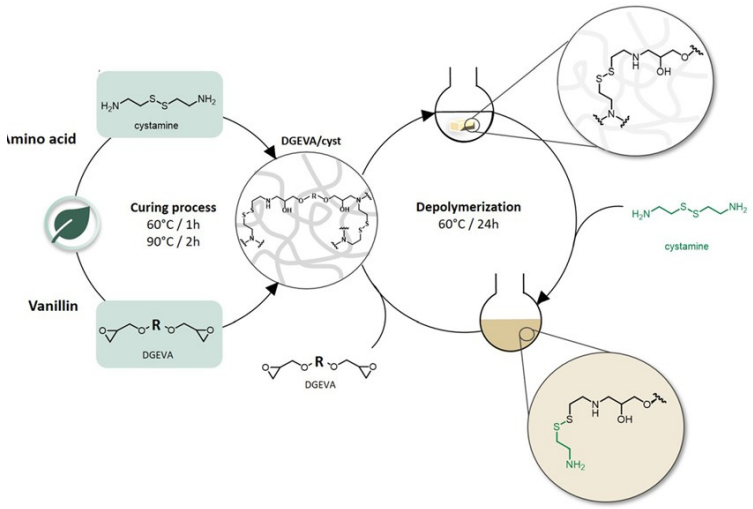


Figure 22 – Curing reaction and depolymerization of DGEVA–Cystamine [25]

2.2.4 Boronic ester bonds without vat photopolymerization

Boronic ester bonds are reversible covalent bonds formed through a reaction between boronic acid and alcohol groups. The electron–deficient character of the boron atom allows the boron–alkoxy bonds to break and reform under suitable temperature and pH conditions, enabling the polymer network to undergo topological rearrangement. This dynamic exchange mechanism provides vitrimers with self–healing, reprocessing, and recycling properties. In bio–based systems, combining renewable raw materials such as epoxidized soybean oil acrylate and castor oil with boronic ester crosslinkers has produced vitrimers capable of room–temperature self–healing, reprocessing, and chemical recycling[3].

2.2.4.1 ESBO–HEA–DBDT

This vitrimer was prepared from a soybean–oil–based acrylate and a diboronic–ester dithiol. Epoxidized soybean oil(ESBO) was first modified with hydroxyethyl acrylate to produce ESBO–HEA. The acrylate groups then reacted with the thiol groups of DBDT through a thiol–acrylate reaction, placing dioxaborolane units inside the crosslinked network. These boronic ester groups exchange by metathesis and allow the network topology to change. The synthesis was described as a one pot, thermally controlled process[26].

The cured network was soft, with a glass–transition temperature of 5.22 °C, and could stretch by roughly 700–1200% depending on the test conditions. Its dynamic response was very fast. The stress–relaxation time was around 15 s at 25 °C and the activation energy was only 8.70 kJ mol^{-1}. Cut surfaces recovered fully within 15 h at room temperature or 4 h at 50 °C. The material also maintained its mechanical response after two reprocessing cycles. Chemical recycling was demonstrated by hydrolysing the boronic ester groups in 95% ethanol and recovering material after solvent evaporation[26].

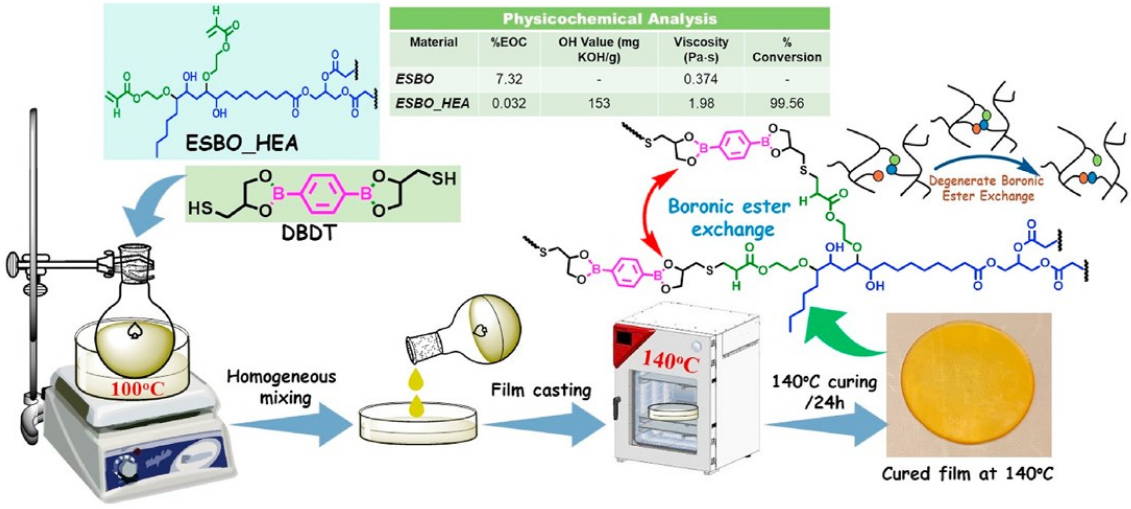


Figure 23 – Preparation of ESBO–HEA–DBDT [26]

The times required to reach the 1/e value in the stress–relaxation tests are:

Temperature	Relaxation time
25 °C	15.6 s
40 °C	12.6 s
60 °C	10.8 s
70 °C	9.6 s

Table 10 – Relaxation time of ESBO–HEA–DBDT [26]

The low–temperature repair behaviour is the main advantage of this system. It avoids the 150–220 °C treatments often needed for transesterification. The same mobility that supports rapid healing also produces a soft material, so the formulation is better suited to flexible parts than to rigid load–bearing structures.

2.2.4.2 ESOA–DBEDT

The ESOA–DBEDT vitrimer was prepared from epoxidized soybean oil acrylate (ESOA) and a diboronic ester dithiol crosslinker (DBEDT). A mixture containing 7.33 g of ESOA and 2.67 g of DBEDT was cured at 120 °C for 24 h through a thermally activated thiol–acrylate reaction. This reaction formed a crosslinked network containing dynamic dioxaborolane groups without requiring a solvent or catalyst. The exchange of these boronic ester groups allows the network to rearrange without permanently reducing its crosslink density [27].

The vitrimer had a glass–transition temperature of 10.5 °C according to DMTA and an activation energy of 29 kJ mol^{-1}. Its tensile response strongly depended on the extension rate. The ultimate strength increased from 0.02 MPa at 10 mm min^{-1} to 1.12 MPa at 500 mm min^{-1}, and the specimen reached approximately 3000% strain without breaking at the highest rate. A mechanical cut healed completely within 6 h at room temperature, while the remaining surface deformation disappeared after 24 h. The material was reprocessed four times by compression moulding at 140 °C under a five–ton load for 10 min, without a

significant reduction in mechanical performance. Chemical recycling was also demonstrated by hydrolysing and dissolving the vitrimer in 90% ethanol overnight, followed by solvent casting to recover the material. Biochemical oxygen demand tests additionally showed that biodegradation in seawater began after approximately 3–4 days [27].

Chapter 3: Filler materials

Fillers in vitrimer formulations do more than improve mechanical performance. Depending on their chemistry and morphology, they may promote heat transfer, introduce electrical or magnetic responsiveness, or provide functional groups that influence dynamic bond exchange. Cellulose–derived fillers are a good example, since they can reinforce the matrix while contributing surface hydroxyl groups. The final response of the composite, however, is governed not only by the intrinsic properties of the filler, but also by its loading, surface chemistry, dispersion, and effect on polymer–chain mobility. These factors often determine whether an improvement in stiffness or functionality is achieved at the expense of stress relaxation and repair.

3.1 Hexagonal boron nitride (hBN)

Hexagonal boron nitride was introduced mainly to improve corrosion protection and assist heat distribution during thermal repair in the epoxy vitrimer coating. Its plate like particles create a more difficult path for water and chloride ions moving toward the steel substrate and the high thermal conductivity of hBN can promote a more uniform temperature across the coating. hBN is not included in the exchange mechanism and also it doesn't work as a catalyst. Its role in the system is strengthening the protective barrier and helping to establish the thermal conditions required for self–repair[28].

The coating was prepared from a Diglycidyl ether of bisphenol (DGEBA) based epoxy cured with 2–aminophenyl disulfide (2–APD), which introduced dynamic disulfide bonds into the network. hBN was then added at 0.5, 1.0, and 1.5 wt%[28]. After application to steel substrates, the coatings were evaluated in terms of surface morphology and roughness, water contact angle, pull–off adhesion strength, thermal stability, self–repair behavior, and corrosion resistance.

Thermal repair was analyzed by heating scratched coatings at 120 °C for 1 h. Under these conditions, the unfilled epoxy vitrimer reached a self repair efficiency of 31%, whereas the formulation containing 1 wt% hBN reached 88%. Increasing the filler content to 1.5 wt% reduced the efficiency to 56%[28]. This decline associated with particle agglomeration and restricted chain mobility at the higher loading. The result shows that adding more filler does

not necessarily improve repair performance and that an appropriate loading must be determined.

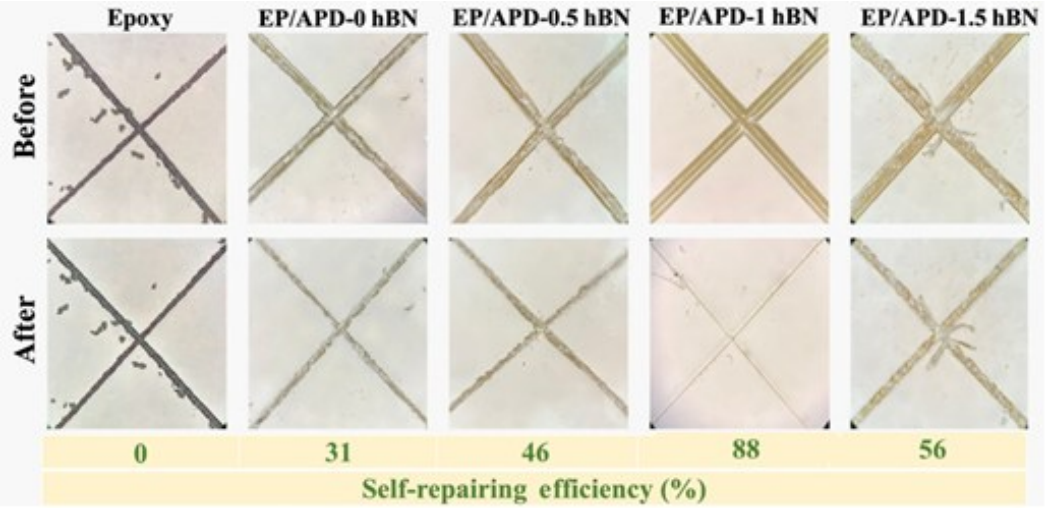


Figure 24 – Self–repairing performance of hBN [28]

A similar optimum was observed in the corrosion measurements. The coating containing 1 wt% hBN showed the lowest corrosion rate, which decreased from 8.79×10^{-4} to 0.50×10^{-4} mm year^{-1}, corresponding to a reduction of approximately 94%. Its water contact angle also increased from 83.8° to 96.9°, indicating a more hydrophobic surface. Adhesion strength to substrate material also continued to rise with filler content. For the unfilled coating is is measured as 850 kPa and for the1.5 wt% hBN, the value was 1310 kPa . In this case, the composition with 1.5 wt% hBN has the highest adhesion strength while 1 wt% hBN 1150 kPa but it was not the one that gave the best self–repair and corrosion performance together [28].

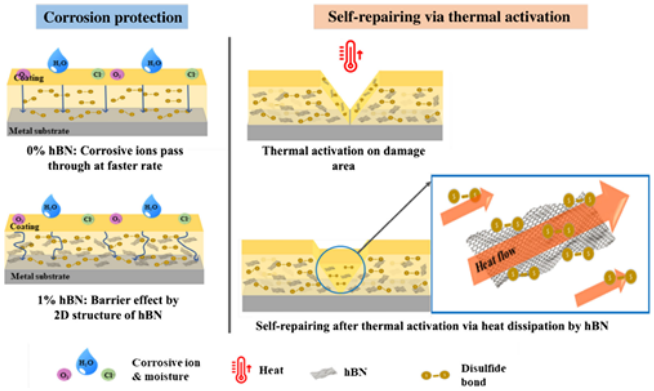


Figure 25 – Shematic representation of corrosion protection and self repairing via thermal activation [28]

3.2 Magnetite nanoparticles (Fe_3O_4)

Magnetite nanoparticles were incorporated into a photocurable dynamic network to combine magnetic responsiveness with thermally activated repair. Once printed, the components could be moved and positioned without physical contact by applying an external magnetic field. Although Fe_3O_4 is often used in systems based on induction heating however that mechanism was not investigated in this work. Repair was instead carried out by heating the specimens in an oven[29].

0 – 6 wt% Fe_3O_4 dispersed in a photocurable thiol–acrylate resin whose network could rearrange through transesterification. Miramer A99 used as catalyst at elevated temperature. Filler addition also had an effect on processability. The viscosity did not increase significantly up to 4 wt% Fe_3O_4. Unfilled resin had a viscosity around 203 mPa·s and it increased to 302 mPa·s at 4 wt% Fe_3O_4 and for the further additions it is meased that 934 mPa·s for 6 wt%[29].

Fe_3O_4 also absorbed the light and slightly reduced the curing rate. After 64 s of irradiation, the acrylate conversion was 85% for the unfilled resin and 76% for the formulation containing 6 wt% Fe_3O_4[29]. At the same time, the glass–transition temperature increased from approximately 45 to 51 °C as the filler content increased. Stress–relaxation measurements at 180 °C did not show significant dependence of the bond–exchange rate on Fe_3O_4 content within the investigated range.

DLP printing was applied most effectively with the formulation containing 4 wt% Fe_3O_4. The printed parts responded to a 1.24 T magnetic field without direct contact. 6 wt% filler was also used in printing but premature gelation became problematic during longer builds, and features below 1 mm could not print. The 4 wt% composition was therefore selected as a practical compromise between printability and magnetic response[29].

Thermal repair was evaluated using a tensile specimen containing a circular hole. A separately printed disc was inserted into the defect, and the assembly was welded at 180 °C for 4 h. The defect free control sample showed tensile strength 11.2 MPa and the sample with a hole showed tensile strength 2.3 MPa. After welding, the strength recovered to 8.1 MPa, equivalent to about 72% of the control value. Recovery of ductility was much more limited, as the ultimate elongation after repair was only 3.9%. The magnetic response was nevertheless largely preserved after the thermal treatment[29].

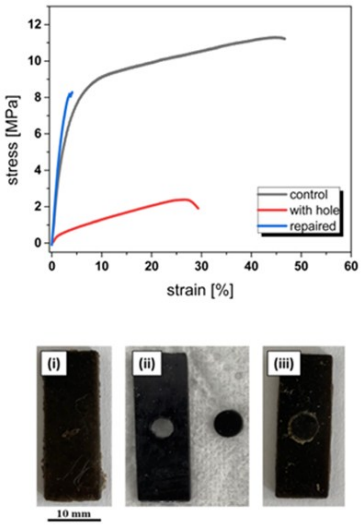


Figure 26 – Stress–strain curve of (i) control sample (ii) sample with hole (iii) repaired sample [29]

This formulation is the only system discussed in this chapter that was directly processed by vat photopolymerization. Its dynamic character was supported by both stress–relaxation and thermal–welding experiments.

3.3 Carbon nanotubes (CNTs/MWCNTs)

Carbon nanotubes can act simultaneously as reinforcing agents and internal heat sources in vitrimer composites. In the studies they were used to improve mechanical performance, convert near–infrared (NIR) radiation into heat, and generate Joule heating under an applied voltage. The resulting local increase in temperature can activate dynamic bond exchange and start a repair process in a damaged region[30].

Bisphenol A diglycidyl ether (DGEBA) epoxy was cured with the bio–based curing agents cashew nut shell liquid (CNSL) and citric acid (CA). Carboxyl–functionalized multi–walled carbon nanotubes (MWCNTs) were added at 0.1, 0.3, and 0.5 wt%. Since the epoxy component was not bio–based, the renewable fraction was limited to the curing agents rather than the entire formulation. At 0.5 wt% CNT, the storage modulus at 0 °C increased from 5773 to 8602 MPa, and the glass–transition temperature increased 27.3 to 30.6 °C[30].

Self healing was activated by exposing the specimens to NIR light at 1.6 mW cm^{-2} for 1 h. The nanotubes converted the absorbed radiation into heat and assisted transesterification within the network[30]. Based on the reduction in scratch width, the self–healing efficiency increased from 31% in the CNT–free material to approximately 93% at 0.5 wt% CNT.

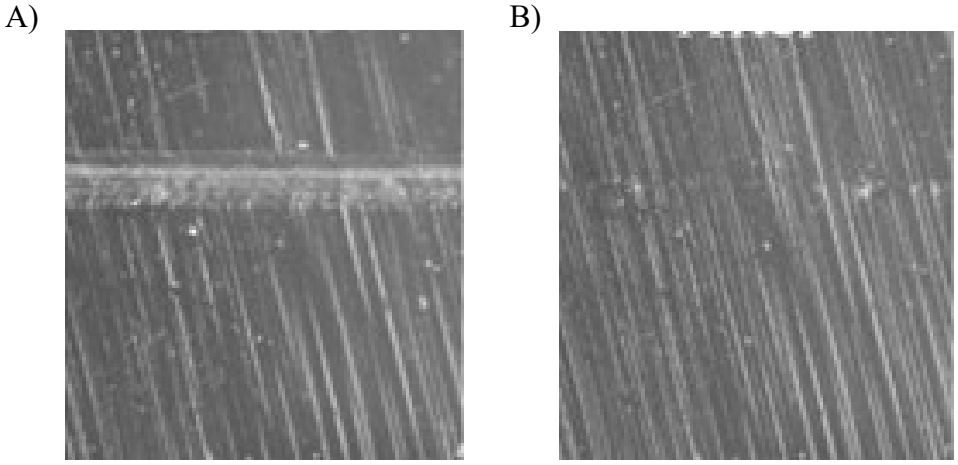


Figure 27 – A) 0.5 wt% CNT before light treatment B) 0.5 wt% CNT after light treatment [30]

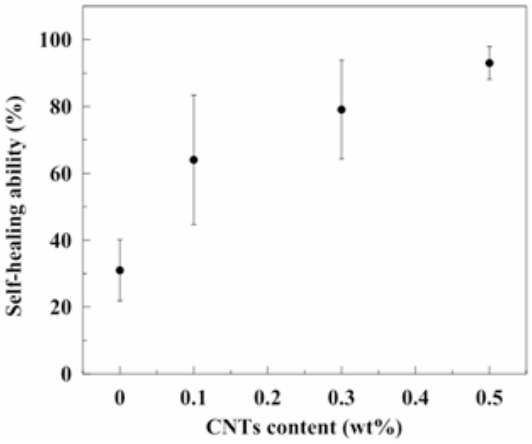


Figure 28 – Self healing ability with different weight ratios [30]

The same formulation also performed as an anticorrosion coating. After 7 d of immersion in 3.5 wt% NaCl, the coating containing 0.5 wt% CNT provided a protection efficiency of 99.99%. These mechanical and barrier improvements were accompanied by slower network dynamics[30]. Increasing the CNT content restricted chain mobility, increased the apparent activation energy of stress relaxation, and slowed bond exchange. However, CNTs enhanced NIR–triggered repair through photothermal heating even though they made the network itself less mobile.

In another experiment, CNT sheets used to trigger repair electrically. The sheets were placed on the surface of a CNT-containing liquid-crystalline elastomer film based on transesterification. Their role differed from that of a conventional dispersed filler. The aligned sheets formed a continuous conductive pathway along the film surface and enabled rapid electrothermal heating[31].

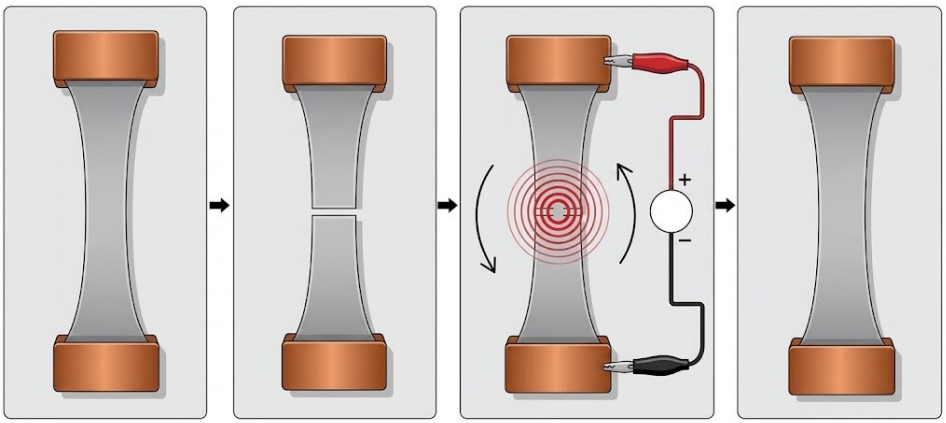


Figure 29 – Self healing mechanism with Joule heating

When 13 V (1.18 V mm^{-1}) was applied across the film, the temperature reached about 180 °C within 10 s [31]. Holes and scratches closed within roughly 3 min, and the repaired film retained a mechanical response close to that of the original material. Electrical conductivity was explained with the CNT sheets re–established contact, whereas mechanical repair resulted from transesterification–driven network rearrangement. This system was also able to act as repairable actuators and supercapacitors.

3.4 Cellulose–based nanofillers (CNCs/CNFs)

Cellulose nanocrystals (CNCs) and cellulose nanofibers (CNFs) are renewable nanofillers capable of reinforcing polymer networks at relatively low loadings. Their surface hydroxyl groups can provide additional reaction sites to transesterification based systems. However, the two studies reviewed shows that similar surface chemistry does not necessarily lead to the same effect on network dynamics. CNCs supplied additional reactive sites and promoted vitrimerization while CNFs mainly restricted chain mobility and slowed stress relaxation[32][33].

3.4.1 Cellulose nanocrystals (CNCs)

The CNC study adopted a mechanochemical route to convert cured epoxy–anhydride waste into a reprocessable vitrimer. The cured epoxy was first broken into small pieces, ball–milled with CNCs and then reshaped by hot pressing with the addition of and zinc acetate catalyst. In this process, hydroxyl groups on the CNC surface provided additional reaction sites for transesterification with ester groups already present in the epoxy network[32].

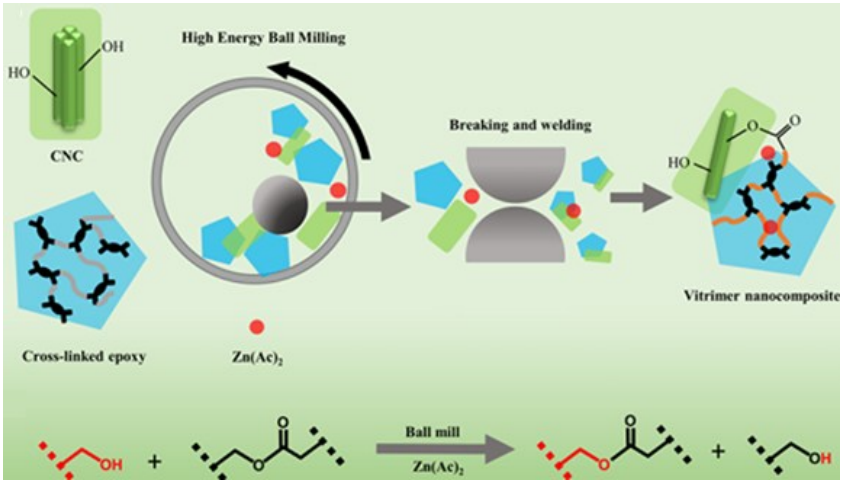


Figure 30 – Miling of CNC and combining with zinc acetate catalyst [32]

Experiments clarified the separate roles of the filler and catalyst. Milled epoxy containing zinc acetate alone could not be reproduced because the original network contained too few free hydroxyl groups. CNC addition without the catalyst was also insufficient. Reprocessing became effective only when the CNC hydroxyl groups and zinc catalyst were used together. Increasing the CNC content, accelerated stress relaxation at 200 °C while the relaxation with 3 wt% CNC was around 4400 s and it reduced around 1100 s at 15 wt% CNC. [32].

The reprocessed composite containing 15 wt% CNC retained a glass–transition temperature of 158 °C, close to the 152 °C value of the original epoxy. At the same time, Young's modulus increased from 1.74 to 2.48 GPa and tensile strength from 68 to 93 MPa[32]. Welding performed by joining two pieces at 200 °C for 30 min, while reshaping, repeated grinding and hot pressing, and shape–memory behavior were also confirmed. CNCs

therefore served a dual purpose in this system, promoting network exchange while increasing mechanical properties of reprocessed material.

3.4.2 Cellulose nanofibers (CNFs)

The CNF study focuses on a transesterification based epoxy vitrimer prepared from diglycidyl ether of bisphenol (DGEBA), sebacic acid, and $Zn(acac)_2$. To examine the effect of the curing method on CNF dispersion, a composite containing 0.5 wt% CNF was prepared using two different methods. In static curing, the components were first mixed at room temperature and then cured at 180 °C for 2 h without further mixing. In dynamic crosslinking, the components were crosslinked at 180 °C under continuous shear in a torque rheometer. The continuous shear improved CNF dispersion and prevented aggregation during curing. The dynamic method was then used to prepare composites containing 0.25–1.0 wt% CNF. The fibers remained uniformly dispersed at loadings up to 0.75 wt%, while serious aggregation occurred at 1.0 wt%[33].

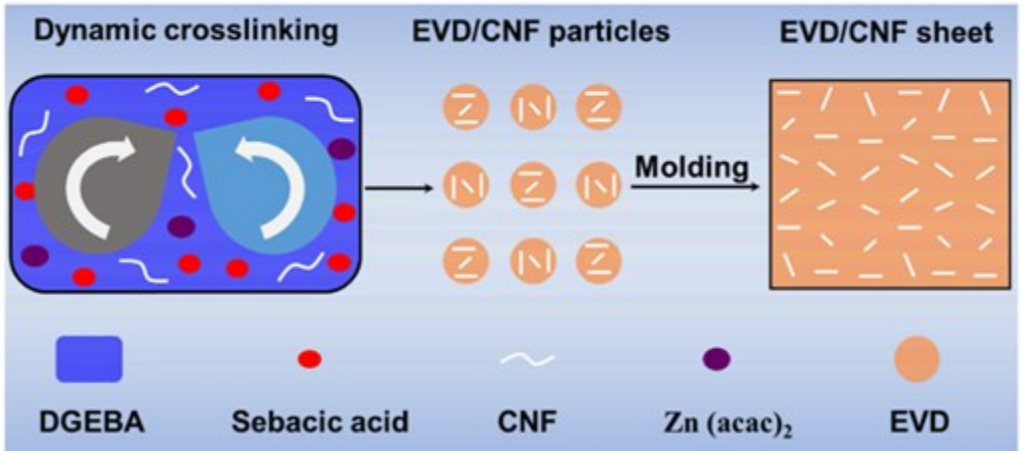


Figure 31 – Illustration of CNF matrix [33]

The strongest mechanical response was obtained at 0.75 wt% CNF. At this loading, the tensile strength reached 12.42 MPa and Young's modulus 8.27 MPa, corresponding to 2.26

and 3.61 times the respective values of the unfilled vitrimer. Raising the CNF content to 1 wt% reduced both properties and also caused to aggregation[33].

Mechanical reinforcement did not coincide with faster network exchange. At 180 °C, the characteristic relaxation time increased from 450 s for the unfilled vitrimer to 1132 s at 0.75 wt% CNF and 1605 s at 1 wt%[33]. The fibers therefore restricted polymer–chain motion rather than accelerating transesterification. All of the composites still exhibited clear stress relaxation and were considered thermally reprocessable. Although CNF is a bio–based filler while the DGEBA–containing matrix was not fully bio–based.

3.5 Functionalized silica

Surface functionalization is particularly important in silica filled vitrimers because the filler matrix interface affects both reinforcement and network mobility. Strong interfacial interactions can improve load transfer but may also restrict the chain motion needed for stress relaxation and self–healing. To examine this balance, unmodified silica (U–Silica) is compared with epoxy functionalize (EP–Silica) and thiol functionalized silica (SH–Silica) in the same disulfide based epoxy vitrimer[34].

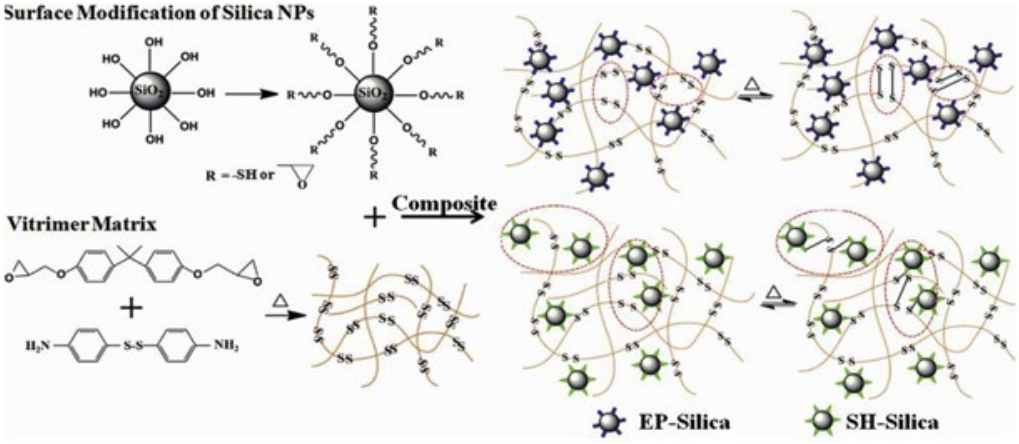


Figure 32 – Scheme of synthesis of functionalized silica [34]

At a loading of 5 wt%, both functionalized fillers dispersed more uniformly than unmodified silica and formed stronger interactions with the matrix. The tensile modulus and tensile strength of the unfilled vitrimer were 598 MPa and 58.5 MPa, respectively[34]. Epoxy–functionalized silica increased these values to 715 MPa and 66.2 MPa, while thiol–functionalized silica produced values of 689 MPa and 64.9 MPa. The epoxy–functionalized particles therefore provided slightly greater mechanical reinforcement.

The distinction between the two surface chemistries became clearer in the stress–relaxation experiments. At 180 °C, the characteristic relaxation time was 52 s for the unfilled vitrimer and 57 s for the composite with 5 wt% thiol–functionalized silica, but increased to 109 s with 5 wt% epoxy–functionalized silica[34]. The thiol surface showed better interface for dynamic exchange. It did not accelerate relaxation relative to the unfilled network, but caused only a minor delay while the epoxy–functionalized particles restricted network mobility much more strongly.

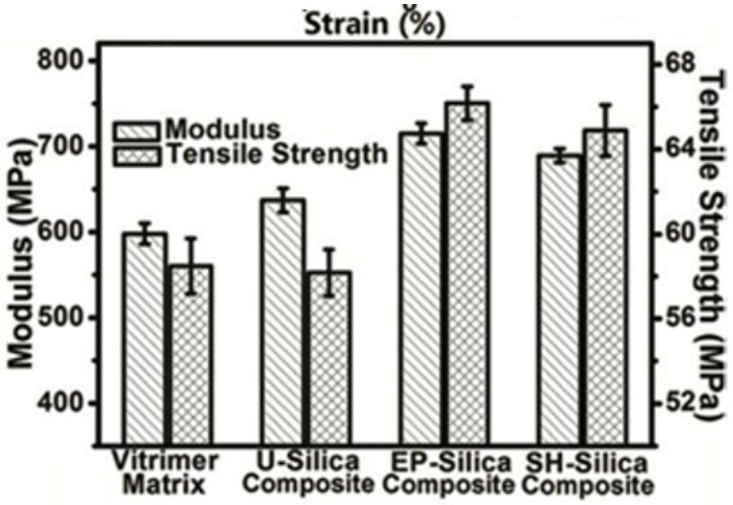


Figure 33 – Mechanical properties of vitrimer matrix and silica composites [34]

The self healing results followed the same trend for fractured surface. After 120 min at 180 °C, the efficiency calculated from the recovered tensile strength was 78.9% for the unfilled vitrimer, 78.1% for the thiol–functionalized composite, and 63.7% for the epoxy–functionalized composite. Thiol functionalization kept a level of self–healing close to that

of the neat network while still improving the mechanical properties. More broadly, the study shows that appropriate surface chemistry can provide a better balance between reinforcement and dynamic performance[34].

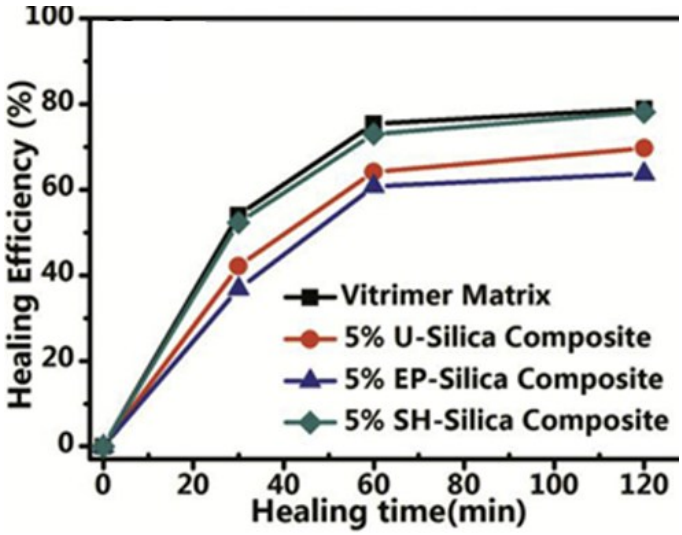


Figure 34 – Healing efficency of vitrimer matrix and silica composites [34]

3.6 Graphene oxide (GO)

Graphene oxide was incorporated into a disulfide–based epoxy vitrimer to improve its flexural properties and enable self–healing at comparatively low temperatures.

The effect of GO on the glass–transition temperature depended strongly on filler loading. At 1 wt%, the value decreased from 64 to 53 °C according to DMA and from 62 to 48 °C according to DSC. This reduction attributed to additional free volume at the GO–epoxy interface, which allowed greater chain mobility. Beyond 1 wt%, the glass–transition temperature began to rise again, most likely because increasing agglomeration changed interfacial effect[35].

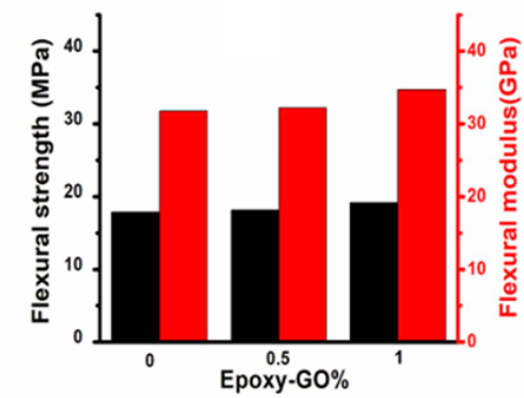


Figure 35 – Flexural strength and modulus of Epoxy–GO [35]

The 1 wt% GO formulation also showed a 7.1% increase in flexural strength and a 9.4% increase in flexural modulus relative to the unfilled vitrimer. For repeated self–healing tests, cut specimens were held together at 80 °C for 5 min. The unfilled material recovered 73% of its flexural modulus in the first cycle and 60% in second cycle while the GO composite reached 88% and 80% respectively[35]. Additionally it is reported that the 1 wt% GO formulation could exhibit low–temperature self–healing at 60 °C.

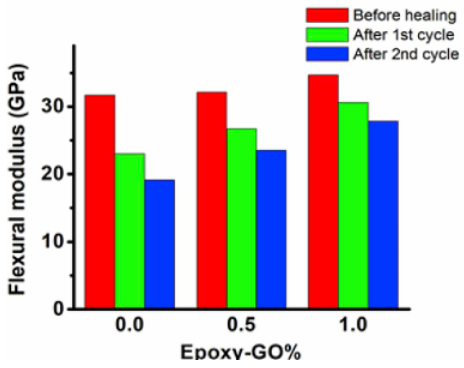


Figure 36 – Flexural modulus of Epoxy–GO before healing and after healing cycles [35]

GO also improved shape recovery. The unfilled vitrimer recovered approximately 95% of its original shape, whereas the composites containing 0.5 and 1 wt% GO achieved 100% recovery. Among the tested formulations, the 1 wt% GO composite provided the best

overall balance: it exhibited a lower glass–transition temperature, complete shape recovery, and a 7.1% higher flexural strength than the unfilled vitrimer.

3.7 Activated carbon

Activated carbon is a porous biofiller that can be produced from agricultural waste. In this study[36], activated carbon derived from sugarcane bagasse was added to a disulfide–based epoxy vitrimer to improve mechanical performance and reduce the temperature required for self–healing. A part from the bio based filler, both the epoxy resin and the disulfide curing agent were synthetic.

Activated carbon was incorporated at 0.1, 0.2, 0.5, 1, and 2 wt% and 1 wt% formulation selected for more detailed analysis. At this loading, the glass–transition temperature decreased from 64 to 59 °C, while the storage modulus increased. The flexural modulus was also approximately 35% higher than the unfilled vitrimer. In this work "EP–p" used for epoxy without activated carbon and "EP–1" used for the filler added formulation[36].

Samples	Storage modulus (GPa)	Flexural strength (MPa)	Flexural strain at break (mm mm^{-1})	Flexural modulus (GPa)	Activation energy (Ea) (kJ mol^{-1})	Topology transition temperature (Tv) (°C)	Before healing (GPa)	After healing 1st (GPa)	After healing 2nd (GPa)
EP–p	39.7	18.0	0.06	32.1	59	19	32.1	23.4	19.5
EP–1	57.5	18.1	0.05	43.3	79	43	43.3	36.9	33.7

Table 11 – Mechanical properties of EP–p and EP–1 [36]

The reduction in glass–transition temperature did not correspond to faster stress relaxation. At 70 °C, the relaxation time increased from 40.8 s for the unfilled vitrimer to 129.6 s for the composite containing 1 wt% activated carbon, indicating that the filler restricted chain mobility[36]. Even if activated carbon lowers chain mobility, lower glass–transition temperature made repair possible under lower temperatures, the unfilled vitrimer required 80 °C for 5 min, whereas the activated–carbon composite could be healed at 70 °C over the same period.

Self–healing efficiency, determined from the recovery of flexural modulus, increased from 73% for the unfilled vitrimer to 85% for the activated–carbon composite in the first cycle. In the second cycle, the efficiency values were 60% and 78%. These findings indicate that activated carbon did not directly accelerate disulfide exchange. It facilitated repair at lower temperature by modifying the thermal and mechanical response of the network.

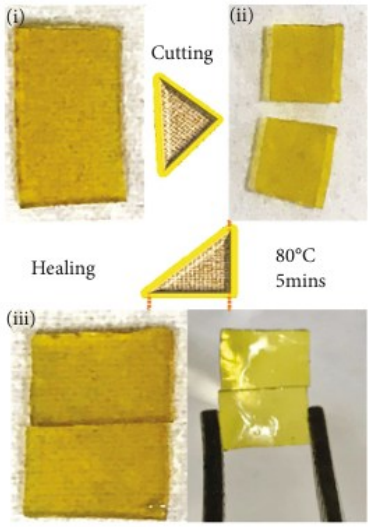


Figure 37 – Healing of epoxy vitrimer [36]

3.8 Amine–functionalized POSS (POSS–NH_2)

Amine–functionalized polyhedral oligomeric silsesquioxane (POSS–NH_2) was used as a nanofiller in a partially bio–based polymethacrylate vitrimer. The polymer matrix consisted of poly(AAEMA–stat–IBOMA), while vegetable–oil–derived Priamine acted as the crosslinker. The two amine groups of Priamine reacted with the β–ketoester groups of AAEMA to connect different polymer chains through dynamic vinylogous urethane bonds. These bonds undergo transamination at elevated temperatures and allow the network to rearrange[37].

In the Table 12, Vitrimer – S indicates the formulation without the filler and Composite – 5, 10, 20 indicates the formulations with different filler ratios.

Resins	POSS–NH_2 (wt%)	POSS–NH_2 : AAEMA (mol mol^{-1})	Priamine : AAEMA (mol mol^{-1})
Vitrimer – S	0	0:1	0.7:1
Composite – 5	5	0.02:1	0.7:1
Composite – 10	10	0.05:1	0.7:1
Composite – 20	20	0.09:1	0.7:1

Table 12 – Different POSS–NH_2 ratios in different resins [37]

The greatest improvement was obtained with 20 wt% POSS–NH_2. At this loading, Young's modulus increased from 96 to 176 MPa, stress at break increased from 2.54 to 4.96 MPa, and the decomposition temperature increased from 225 to 255 °C. However, POSS–NH_2 also restricted polymer–chain mobility. At 110 °C, the relaxation time increased from 9 s for the unfilled vitrimer to 21 s for the 20 wt% composite, while the apparent activation energy increased from 56 to 70 kJ mol^{-1}[37]. Therefore, POSS–NH_2 improved the mechanical and thermal properties but slowed the dynamic exchange process.

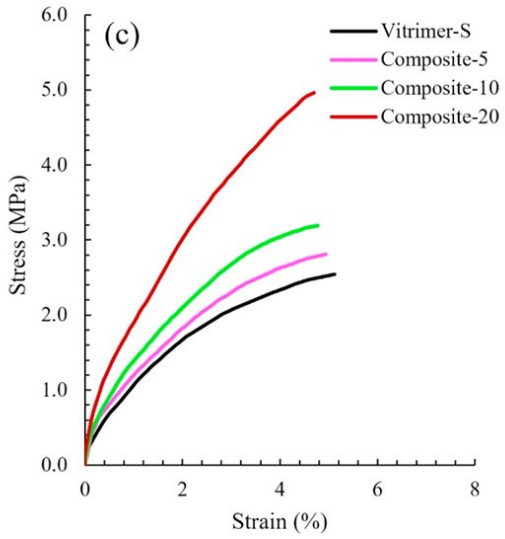


Figure 38 – Stress–strain graph of the resins [37]

Mechanical reprocessing was performed by grinding the specimens and hot–pressing them at 125 °C under a load of 14 t for 6 h. After three reprocessing cycles, the modulus of the 20 wt% composite decreased from 176 to 155 MPa and its stress at break decreased from 4.96 to 3.99 MPa. The average recovery of its mechanical properties was approximately 88%. In a separate experiment, the unfilled Vitrimer–S network was dissolved using excess butylamine at 65 °C, and the original copolymer was subsequently recovered by precipitation in methanol[37]. However, this material was not produced by vat photopolymerization, the study demonstrates how a covalently attached POSS nanofiller can improve a partially bio–based vitrimer while maintaining its reprocessability.

Chapter 4: Results and Discussion

Based on the obtained data, it was observed that different vitrimer mechanisms and resin systems exhibited significantly different properties. Even when the same resin system was used, changing the component ratios also changed the material properties. Specifically, significant differences were observed among the resins in terms of glass transition temperature (*Tg*), topological freezing temperature (*Tv*), relaxation time and mechanical properties. Furthermore, different vitrimer mechanisms such as transesterification, imine, and boronic ester displayed completely distinct behaviors under heat and during network rearrangement. These differences are the main factors shaping the thermal and mechanical responses of the systems.

According to the data analyzed in this study and summarized in Table 13 and Table 14, topological freezing temperature (*Tv*) values span a very wide range. The recorded *Tv* values range from a minimum of -196 °C to a maximum of 118 °C. This broad spectrum provides significant flexibility in designing vitrimer structures. Depending on the desired application and the environmental temperature conditions, the most suitable vitrimer system from this range can be selected. Systems with low *Tv* values are preferable when low temperature processability is desired, while network structures with higher *Tv* values can be chosen for structural applications requiring high temperature resistance. In this case, vitrimer materials can be designed to their spesific uses.

Beside these wide range of resins, also addition of the filler materials into vitrimer formulations offers significant advantages beyond just mechanical reinforcement. Depending on their specific chemistry and morphology, fillers can introduce thermal, electrical or magnetic responsiveness, and even actively participate in the dynamic bond exchange. For instance, thermally conductive fillers like hexagonal boron nitride (hBN) facilitate uniform heat distribution during thermal repair, while carbon nanotubes (CNTs) used for Joule heating. Some fillers directly influence network mobility and exchange kinetics such as cellulose nanocrystals (CNCs) can accelerate transesterification by providing additional surface hydroxyl. Therefore, the successful integration of fillers into vat-printable bio-based vitrimers can expand the range of usability and makes possible to do adjustments to resins for desired properties.

Resins	Tg (°C)	Tv (°C)	Reprocessing Conditions	Relaxation Time (τ*)	Tensile Strength (MPa)	Tensile Modulus (MPa)	Storage Modulus (MPa)	Viscosity (mPa·s)
Transesterification								
GDGDA–THFMA (60G/40T)	0	50	180 °C, 5 h, Welding	180–220 °C, 5.5 h - 2.3 h	4.9 (Original) 26 (Welded)	12 (Original) 550 (Welded)	224.5	1394
DGEVADMA–HPPA (20D/80H)	12	118	180 °C, 1 h, Welding	160 – 200 °C, 43 min - 22 s	150 (Original) 300 (Welded)	13 (Original) 9 (Welded)	269.6	9354
HPPA–MCC (HC10)	43.7	-	180 °C, 24 h, Heat treatment	150 - 170 °C, ~30 min	5 (Original) 30 (Heat treatment)	43 (Original) 1815 (Heat treatment)	4	~500
AESO–AEUG–EUGP (BG/Te)	64-68	-	-	180 – 220 °C, 13 min - 833 min	10.5 (Original)	1.4 (Original)	10^9	4000
THFMA–AESO–HPPA (40THFMA)	7	66	200 °C, 3 bar, 1 h, divided to pieces and remolded 180 °C, 4 h, welding	160 – 220 °C, 145 min - 16 min	0.27 (Original) 0.50 (Welded)	0.75 (Original) 6 (Heat treatment)	57.19	413
DPEPA–GDGDA–GLYFOMA–RTE (N5)	68	108	Hot press (3 Cycle)	160 – 200 °C, 225 min - 35 min	16 (Original) 1.5 (Cycle 3)	17 (Original) 8.5 (Cycle 3)	22.96	381
HPPA–AESO (9HPPA)	23	72	180 °C, 5 MPa, 1 h, Powdered and heated with pressure	160 – 200 °C, 172 min - 11.5 min	1.39 (Original) 0.43 (Recycled)	3.45 (Original) 6.86 (Recycled)	23.25	332
AERO–HPPA–GDGDA (AERO30)	18	-	200 °C, 2 h, Powdered hot pressed	200 °C, 10 min	0.86 (Original) 0.43 (Cycle 3)	7.6 (Original) 7.0 (Recycled)	60	458–939
AELO–EGMP–TMP3MP–DMEP	-18 (EGMP) -10 (TMP3MP)	-	180 °C, 4 h, Heat treatment	180 °C, 22 min (EGMP), 77 min (TMP3MP)	0.58 (EGMP) 1.18 (TMP3MP) / 1.0 (EGMP R) 1.13 (TMP3MP R)	4.0 (EGMP) 4.5 (TMP3MP) / 1.0 (EGMP R) 1.3 (TMP3MP R)	-	2.1 (EGMP) 11.9 (TMP3MP)
Imine Bonds								
HMDA–MAV–EGPMA (UV50 / UV25)	97 (UV50) 73 (UV25)	38.4 (UV50) 32.0 (UV25)	160 °C, 5 min, 5 MPa, Powdered	140 °C, 49 s (UV50), 139 s (UV25)	39 (UV50) 37 (UV25)	3045 (UV50) 2940 (UV25)	2412 (UV50) 2614 (UV25)	-
CROSS–BDG–IBOMA (CROSS-5)	63-76	-	150 °C, 5 min, 40 kN,	60 – 180 °C, 100 s - 6 s	~33 (Original) ~30 (Cycle 3)	~1400 (Original) ~1350 (Cycle 3)	-	< 7000
Disulfide Bonds								
CMAV–IBA (R2)	63.2	-	80 °C, 48 h, Chemically recycled	-	31.4 (Original) 24.4 (Recycled)	1860 1420	-	25

Table 13 – Summary table of vat photopolymerization resins

Resins	Tg (°C)	Tv (°C)	Reprocessing Conditions	Relaxation Time (τ*)	Tensile Strength (MPa)	Tensile Modulus (MPa)	Storage Modulus (MPa)	Viscosity (mPa·s)
Transesterification Bonds Without Vat Photopolymerization								
FEP–FEHBP–CA (10 phr)	94	110	140 °C, 30 min, 5.0 Mpa	140 °C, 45 s	126.4	~2400	~2600	-
ESO–GL (R = 0.5)	49	69	200 °C, 135 min, 200 kg/cm²	180 - 200 °C, 23 min - 7 min	3.1 (Original) 1.4 (Recycled)	2483 (Original) 2366 (Recycled)	2200	-
Imine Bonds Without Vat Photopolymerization								
PV–1071 and PV–1074	32.2 (PV1071) 30.2 (PV1074)	87 (PV1071) 75 (PV1074)	120 °C, 6 min 10 Mpa	80-120 °C, 40 s - 22 s (1071), 26 s-17 s (1074)	5.48 (PV1071) 5.09 (PV1074)	4.90 (PV1071) 3.54 (PV1074)	5.32 (PV1071) 5.76 (PV1074)	-
Disulfide Bonds Without Vat Photopolymerization								
DGEVA–Cystamine (cyst5 / cyst10)	51 (cyst5) 53 (cyst10)	-	60 °C (1h) + 90 °C (2h) Curing or hot press	140 °C, 367s (cyst5 R), 341s (cyst10 R)	-	-	3457 (cyst5 R) 3709 (cyst10 R)	-
Boronic Ester Bonds Without Vat Photopolymerization								
ESBO–HEA–DBDT	5.22	-196	140 °C, 5 min, 3 tons/m²	25-70 °C, 15.6s-9.6s	0.05 - 0.15	0.05 - 0.10	8.06	-
ESOA–DBEDT	10.5	-121	140 °C, 10 min, 5 ton	60-120 °C, 4.22s - 0.86s	0.02 - 1.12	0.05 - 2.20	0.2	-

Table 14 – Summary table of resins without vat photopolymerization

In addition to resin systems and fillers, the tool used for printing is highly important because even if vat photopolymerization method is used, there are many types of vat printing methods that effects resolution, printing speed, accuracy and volume[38]. Stereolithography (SLA) is the first and most well-known example, using an ultraviolet (UV) laser to scan the resin surface for curing[39]. Even if SLA offers high precision, the printing time increases depending on the part size because the laser scans the cross-section point by point. Digital Light Processing (DLP), on the other hand, projects the entire image of a single layer simultaneously using a digital projector and micromirrors (DMD)[38]. This keeps the curing time per layer constant, regardless of the part size or quantity, offering a distinct speed advantage over SLA. Liquid Crystal Display (LCD) technology also cures the entire layer at once like DLP but uses an LED array and an LCD screen as a mask[39]. Since LCD screens are cheaper, these printers are more accessible. However, their resolution is relatively lower due to optical convergence issues, and the screens have a limited lifespan. Continuous Liquid Interface Production (CLIP) utilizes an oxygen-permeable window to prevent the resin from adhering to the bottom of the tank (creating a

dead zone), allowing the platform to move continuously upwards and achieving much higher speeds than other VPP methods[40]. In final, Two-Photon Polymerization (TPP) uses ultrashort pulsed lasers, enabling polymerization only in the extremely small focal volume of the laser. TPP provides sub-micrometer resolution, making it possible to produce ultra-precise structures like photonic devices or micro-medical parts, but the printing speed is quite slow, and the printable volume is highly restricted[39].

Technology	XY Res.	Surface	Volume	Material	Advantages	Disadvantages	Applications
SLA	25-50 µm	>7 nm	10^3-10^6 cm^3	Photocurable resin	High accuracy and isotropy.	High cost, slow speed.	Lenses, contacts, optical fibers
DLP	10-50 µm	>7 nm	10^3-10^6 cm^3	Photocurable resin	Fast for multiple parts, accurate.	Resolution drops as area expands	Lenses, waveguides, fibers
LCD	40-50 µm	>10 nm	10^3-10^6 cm^3	Photocurable resin	Fast speed, low equipment cost.	Lower resolution, short screen life.	Lenses, optical fibers, waveguides
CLIP	30-50 µm	>10 nm	10^3-10^7 cm^3	Photocurable resin	Very high speed, continuous print.	Complex operation.	Lenses, optical fibers, waveguides
TPP	Sub-µm	<6 nm	Very small	Photoresist / Photocurable resin	Ultra-high nanoscale resolution.	Very slow, restricted volume.	Micro-lenses, fiber tips, resonators

Table 15 – Comparison of vat photopolymerization printers[39]

Chapter 5: Conclusion

Recent studies have shown that raw materials obtained from renewable resources, such as vanillin, soybean oil derivatives, glycerol, and cellulose, can be used in vitrimer systems. One of the main advantages of these materials is that they reduce dependence on petroleum-derived raw materials. Like thermosets, vitrimers have permanently crosslinked structures; however, their main difference is their ability to rearrange without losing the crosslinked network because of the dynamic covalent bonds within their structure. In some of the systems examined, raw materials or oligomers could be recovered through chemical depolymerization. Other systems were mechanically reprocessed under heat and pressure after being divided into small pieces. Their mechanical properties were kept to different degrees after these processes but the same level of property recovery was not achieved in every system. In addition, the ability to print some vitrimer resins using vat photopolymerization techniques such as DLP or LCD enables the production of complex, high-resolution geometries with limited material waste.

The literature review examined different vitrimer mechanisms, including transesterification, imine exchange, disulfide exchange, and boronic ester metathesis. Transesterification was found to be the most widely developed mechanism among the bio-based vat-printable systems evaluated in this thesis. This mechanism is based on an exchange reaction between ester and hydroxyl functional groups. The presence of these groups in glycerol, vegetable oil, and cellulose derivatives, or their introduction into these raw materials through chemical functionalization, facilitates the development of transesterification-based resins. However, imine, disulfide, and boronic ester mechanisms were also showed high dynamic performance. In particular, stress relaxation within approximately 10 seconds was observed in some imine and boronic ester systems. In addition to systems that were actually printed using DLP or LCD, systems that have not yet been processed by vat photopolymerization but show rapid stress relaxation, self-healing, or reprocessing properties were examined separately because of their potential for future photocurable resin studies.

In addition to the effects of the monomers, crosslinkers, and reactive diluents within the resin, the effects of filler materials on mechanical performance, thermal response, and self-healing behaviour were also evaluated. The selection of a filler depends on the properties required from the material. Due to its high thermal conductivity, hBN contributes to a more

uniform distribution of heat within the material and creates thermal repair conditions. Two different heating approaches were observed in CNT-containing systems. Dispersed CNTs converted NIR light into heat and enabled photothermal healing, while conductive CNT sheets generated Joule heating under an electric current and produced the temperature required for bond exchange. In the functionalized silica study, the use of epoxy- and thiol-functionalized silica increased the mechanical properties but did not accelerate stress relaxation. Thiol-functionalized silica caused only a minor delay, whereas epoxy-functionalized silica restricted chain mobility more strongly and increased the relaxation time to a greater extent. Cellulose nanocrystals provided additional reaction sites for transesterification through the hydroxyl groups on their surfaces and accelerated bond exchange in the investigated system while cellulose nanofibers restricted polymer-chain mobility and increased the relaxation time. These results show that even cellulose fillers obtained from similar sources can have different effects on network dynamics.

In conclusion, this study evaluated the current status and future application potential of bio-based vitrimer systems in vat photopolymerization. Not all of the formulations examined were fully bio-based. In some systems, only the main monomer, crosslinker, curing agent, or filler was obtained from renewable resources, while other components, such as the reactive diluent, catalyst, and photoinitiator, were petroleum-derived. However, these systems were included because of their bio-based fraction and their potential to be converted into resins with higher renewable content in the future. Vat photopolymerization was evaluated in this study because of its ability to produce highly detailed and complex geometries with limited material waste. Under appropriate loading and dispersion conditions, filler materials can improve mechanical, thermal, or functional performance. However, increasing the filler content may increase viscosity, reduce light penetration, cause aggregation, and restrict the chain mobility required for dynamic exchange. Some reactive fillers may accelerate stress relaxation by providing additional reaction sites. Therefore, the effects of fillers should be evaluated not only in terms of mechanical reinforcement but also for photocuring, network mobility, and bond-exchange kinetics. In this case, bio-based fillers have significant potential for future photocurable vitrimer systems.

Bibliography

[1] W. Denissen, J. M. Winne, and F. E. Du Prez, “Vitrimers: Permanent organic networks with glass-like fluidity,” Jan. 01, 2016, *Royal Society of Chemistry*. doi: 10.1039/c5sc02223a.

[2] N. J. Van Zee and R. Nicolaÿ, “Vitrimers: Permanently crosslinked polymers with dynamic network topology,” May 01, 2020, *Elsevier Ltd*. doi: 10.1016/j.progpolymsci.2020.101233.

[3] A. Mariani and G. Malucelli, “Biobased vitrimers: towards sustainability and circularity,” Jan. 06, 2025, *Royal Society of Chemistry*. doi: 10.1039/d4cc05967k.

[4] A. Mariani and G. Malucelli, “Biobased vitrimers: towards sustainability and circularity,” Jan. 06, 2025, *Royal Society of Chemistry*. doi: 10.1039/d4cc05967k.

[5] A. Bagheri and J. Jin, “Photopolymerization in 3D Printing,” Apr. 12, 2019, *American Chemical Society*. doi: 10.1021/acsapm.8b00165.

[6] U. Shaukat, E. Rossegger, and S. Schlögl, “A Review of Multi-Material 3D Printing of Functional Materials via Vat Photopolymerization,” Jun. 01, 2022, *MDPI*. doi: 10.3390/polym14122449.

[7] M. Pagac *et al.*, “A review of vat photopolymerization technology: Materials, applications, challenges, and future trends of 3d printing,” Feb. 02, 2021, *MDPI AG*. doi: 10.3390/polym13040598.

[8] S. Grauzeliene, A. S. Schuller, C. Delaite, and J. Ostrauskaite, “Development and Digital Light Processing 3D Printing of a Vitrimer Composed of Glycerol 1,3-Diglycerolate Diacrylate and Tetrahydrofurfuryl Methacrylate,” *ACS Appl. Polym. Mater.*, vol. 5, no. 9, pp. 6958–6965, Sep. 2023, doi: 10.1021/acsapm.3c01018.

[9] S. Grauzeliene, M. Kastanauskas, V. Talacka, and J. Ostrauskaite, “Photocurable Glycerol- and Vanillin-Based Resins for the Synthesis of Vitrimers,” *ACS Appl. Polym. Mater.*, vol. 4, no. 8, pp. 6103–6110, Aug. 2022, doi: 10.1021/acsapm.2c00914.

[10] I. Roppolo Sara Bergia, “Politecnico di Torino Characterization of a vitrimer with methacrylate cellulose crosslinker for 3D printing.”

[11] M. Bergoglio *et al.*, “3D-Printed Acrylated Soybean Oil Scaffolds with Vitrimeric Properties Reinforced by Tellurium-Doped Bioactive Glass,” *Polymers (Basel).*, vol. 16, no. 24, Dec. 2024, doi: 10.3390/polym16243614.

[12] S. Grauzeliene, A. S. Schuller, C. Delaite, and J. Ostrauskaite, “Biobased vitrimer synthesized from 2-hydroxy-3-phenoxypropyl acrylate, tetrahydrofurfuryl methacrylate and acrylated epoxidized soybean oil for digital light processing 3D printing,” *Eur. Polym. J.*, vol. 198, Oct. 2023, doi: 10.1016/j.eurpolymj.2023.112424.

[13] A. Navaruckiene, K. Pamakstys, A. Nasiribouyony, V. Sereikaite, V. Varzinskas, and J. Ostrauskaite, “Development of biobased photocurable resin for LCD 3D printing of reprocessable catalyst-free vitrimer,” *Rapid Prototyp. J.*, pp. 1–11, 2026, doi: 10.1108/RPJ-12-2025-0656.

[14] S. Grauzeliene, B. Kazlauskaite, E. Skliutas, M. Malinauskas, and J. Ostrauskaite, “Photocuring and digital light processing 3D printing of vitrimer composed of 2-hydroxy-2-phenoxypropyl acrylate and acrylated epoxidized soybean oil,” *Express Polym. Lett.*, vol. 17, no. 1, pp. 54–68, Jan. 2023, doi: 10.3144/expresspolymlett.2023.5.

[15] S. Greivule, I. Besprozvannaja, M. Porcarello, and S. Gaidukovs, “Reprocessable and Repairable Bio-Based Vitrimers From Acrylated Epoxidized Rapeseed Oil for Additive Manufacturing,” *Macromol. Mater. Eng.*, vol. 311, no. 6, Jun. 2026, doi: 10.1002/mame.70228.

[16] U. Shaukat, B. Sölle, E. Rossegger, S. Rana, and S. Schlögl, “Vat Photopolymerization 3D-Printing of Dynamic Thiol-Acrylate Photopolymers Using Bio-Derived Building Blocks,” *Polymers (Basel).*, vol. 14, no. 24, Dec. 2022, doi: 10.3390/polym14245377.

[17] X. Yang *et al.*, “Efficient transformation of renewable vanillin into reprocessable, acid-degradable and flame retardant polyimide vitrimers,” *J. Clean. Prod.*, vol. 333, Jan. 2022, doi: 10.1016/j.jclepro.2021.130043.

[18] A. Vilanova-Pérez, S. De la Flor, X. Fernández-Francos, À. Serra, and A. Roig, "Biobased Imine Vitrimers Obtained by Photo and Thermal Curing Procedures─Promising Materials for 3D Printing," *ACS Appl. Polym. Mater.*, vol. 6, no. 6, pp. 3364–3372, Mar. 2024, doi: 10.1021/acsapm.3c03234.

[19] J. Stouten *et al.*, "Biobased Photopolymer Resin for 3D Printing Containing Dynamic Imine Bonds for Fast Reprocessability," *ACS Appl. Mater. Interfaces*, vol. 15, no. 22, pp. 27110–27119, Jun. 2023, doi: 10.1021/acsami.3c01669.

[20] Y. Jin, Z. Lei, P. Taynton, S. Huang, and W. Zhang, "Malleable and Recyclable Thermosets: The Next Generation of Plastics," Dec. 04, 2019, *Cell Press*. doi: 10.1016/j.matt.2019.09.004.

[21] G. N. Kamble and S. K. Asha, "Biobased Reprintable Bis-Dynamic Covalent Photopolymer Composition for Digital Light Processing 3D Printing with Self-Healing Properties," *ACS Appl. Polym. Mater.*, vol. 7, no. 3, pp. 1401–1410, Feb. 2025, doi: 10.1021/acsapm.4c03116.

[22] L. Zhong *et al.*, "Closed-Loop Recyclable Fully Bio-Based Epoxy Vitrimers from Ferulic Acid-Derived Hyperbranched Epoxy Resin," *Macromolecules*, vol. 55, no. 2, pp. 595–607, Jan. 2022, doi: 10.1021/acs.macromol.1c02247.

[23] J. Wu, X. Yu, H. Zhang, J. Guo, J. Hu, and M.-H. Li, "Fully Biobased Vitrimers from Glycyrrhizic Acid and Soybean Oil for Self-Healing, Shape Memory, Weldable, and Recyclable Materials," *ACS Sustain. Chem. Eng.*, vol. 8, no. 16, pp. 6479–6487, Apr. 2020, doi: 10.1021/acssuschemeng.0c01047.

[24] Z. Zhou, X. Su, J. Liu, and R. Liu, "Synthesis of Vanillin-Based Polyimine Vitrimers with Excellent Reprocessability, Fast Chemical Degradability, and Adhesion," *ACS Appl. Polym. Mater.*, vol. 2, no. 12, pp. 5716–5725, Dec. 2020, doi: 10.1021/acsapm.0c01008.

[25] S. Guggari, F. Magliozzi, S. Malburet, A. Graillot, M. Destarac, and M. Guerre, "Closed-loop recycling of bio-based disulfide vitrimer via a solvent-and waste-free strategy," *Green Chemistry*, vol. 27, no. 22, pp. 6392–6398, May 2025, doi: 10.1039/d5gc01872b.

[26] C. Bodhak, P. Sahu, and R. K. Gupta, “Sustainable soybean oil acrylate for boronic ester vitrimer: Self-healing, reprocessable and extensive elongation performance,” *Polymer (Guildf).*, vol. 320, Feb. 2025, doi: 10.1016/j.polymer.2025.128095.

[27] A. Zych *et al.*, “Biobased, Biodegradable, Self-Healing Boronic Ester Vitrimers from Epoxidized Soybean Oil Acrylate,” *ACS Appl. Polym. Mater.*, vol. 3, no. 2, pp. 1135–1144, Feb. 2021, doi: 10.1021/acsapm.0c01335.

[28] N. F. Norapandi, R. Roslan, N. Salim, K. F. Chong, and N. H. A. Bakar, “Smart hBN/epoxy vitrimer coating with distinct mechanisms for thermally activated self-repair and corrosion protection,” *J. Coat. Technol. Res.*, 2026, doi: 10.1007/s11998-025-01235-z.

[29] I. Cazin *et al.*, “Digital light processing 3D printing of dynamic magneto-responsive thiol-acrylate composites,” *RSC Adv.*, vol. 13, no. 26, pp. 17536–17544, Jun. 2023, doi: 10.1039/d3ra02504g.

[30] N. Lorwanishpaisarn *et al.*, “Self-healing Ability of Epoxy Vitrimer Nanocomposites Containing Bio-Based Curing Agents and Carbon Nanotubes for Corrosion Protection,” *J. Polym. Environ.*, vol. 30, no. 2, pp. 472–482, Feb. 2022, doi: 10.1007/s10924-021-02213-3.

[31] H. Wang *et al.*, “Electricity-Triggered Self-Healing of Conductive and Thermostable Vitrimer Enabled by Paving Aligned Carbon Nanotubes,” *ACS Appl. Mater. Interfaces*, vol. 12, no. 12, pp. 14315–14322, Mar. 2020, doi: 10.1021/acsami.9b21949.

[32] L. Yue, M. Amirkhosravi, K. Ke, T. G. Gray, and I. Manas-Zloczower, “Cellulose nanocrystals: Accelerator and reinforcing filler for epoxy vitrimerization,” *ACS Appl. Mater. Interfaces*, vol. 13, no. 2, pp. 3419–3425, Jan. 2021, doi: 10.1021/acsami.0c19350.

[33] Y. Ran, Y. D. Li, and J. B. Zeng, “Dynamic crosslinking towards well-dispersed cellulose nanofiber reinforced epoxy vitrimer composites,” *Composites Communications*, vol. 33, Aug. 2022, doi: 10.1016/j.coco.2022.101228.

[34] Z. Huang, Y. Wang, J. Zhu, J. Yu, and Z. Hu, “Surface engineering of nanosilica for vitrimer composites,” *Compos. Sci. Technol.*, vol. 154, pp. 18–27, Jan. 2018, doi: 10.1016/j.compscitech.2017.11.006.

[35] B. Krishnakumar *et al.*, “Catalyst free self-healable vitrimer/graphene oxide nanocomposites,” *Compos. B Eng.*, vol. 184, Mar. 2020, doi: 10.1016/j.compositesb.2019.107647.

[36] B. Krishnakumar *et al.*, “Sugarcane Bagasse-Derived Activated Carbon- (AC-) Epoxy Vitrimer Biocomposite: Thermomechanical and Self-Healing Performance,” *Int. J. Polym. Sci.*, vol. 2021, 2021, doi: 10.1155/2021/5561755.

[37] F. Hajiali, S. Tajbakhsh, and M. Marić, “Thermally reprocessable bio-based polymethacrylate vitrimers and nanocomposites,” *Polymer (Guildf).*, vol. 212, Jan. 2021, doi: 10.1016/j.polymer.2020.123126.

[38] E. Caussin *et al.*, “Vat Photopolymerization 3D Printing in Dentistry: A Comprehensive Review of Actual Popular Technologies,” Feb. 01, 2024, *Multidisciplinary Digital Publishing Institute (MDPI)*. doi: 10.3390/ma17040950.

[39] D. Chekkaramkodi, L. Jacob, M. S. C, R. Umer, and H. Butt, “Review of vat photopolymerization 3D printing of photonic devices,” Apr. 25, 2024, *Elsevier B.V.* doi: 10.1016/j.addma.2024.104189.

[40] F. Zhang *et al.*, “The recent development of vat photopolymerization: A review,” Dec. 01, 2021, *Elsevier B.V.* doi: 10.1016/j.addma.2021.102423.